Surface Modification of a Copper Substrate through the Reaction Chemistry Generated by Pulsed Plasmas in Water

Oberflächenmodifizierung eines Kupfersubstrates duch die Reaktionschemie erzeugt von gepulsten Plasmen in Wasser

Bachelor Thesis

in the
Degree Programm
„Bachelor of Science“
in Physics

at the Faculty of Physics and Astronomy
of the Ruhr-Universität Bochum

by
Fatma-Nur Seferoglu

from
Essen

Bochum 2019

Abstract

Plasmen in Flüssigkeiten bieten vielseitige Anwendungen in der Chemie, Biomedizin und Industrie an. Die chemische Synthese und der Wachstum von Nanopartikeln sind einige dieser Anwendungen. Kupfernanopartikel werden beispielsweise als Katalysatoren in der elektrochemischen Umwandlung von Kohlenstoffdioxid verwendet. Die Eigenschaften von den Katalysatoren können durch chemische Reaktionen, die durch das gepulste Plasma in der Flüssigkeit erzeugt werden, verändert werden. Die Verschlechterung der katalytischen Aktivität in elektrochemischen Zellen ist heutzutage eine große Herausforderung. Gepulste Plasmen in Flüssigkeiten könnten die Kupfernanopartikel auf der Kupferoberfläche reaktivieren, während sie sich in einer elektrochemische Zelle befinden.

In dieser Arbeit wird die Oberflächenstruktur von Kupfersubstraten, die in elektrochemischen Zellen verwendet werden, analysiert. Diese Kupfersubstrate werden mit einem gepulsten Plasma in einer Flüssigkeit behandelt, indem die Plasmaparameter wie Spannung und Frequenz variiert werden. Als Flüssigkeit werden destilliertes Wasser und in destilliertem Wasser gelöstes Kaliumchlorid verwendet. Ein Rasterelektronenmikroskop wird benutzt, um die plasmabehandelten Kupferoberflächen zu veranschaulichen und die Nanopartikel, die sich auf der Kupferoberfläche aufgebaut haben, zu untersuchen. Die chemischen Verbindungen der Nanopartikel werden mittels Röntgenphotoelektronenspektroskopie analysiert.

Die elektrische Leitfähigkeit der Flüssigkeit in der Entladungskammer steigt nach der Plasmabehandlung von Kupfersubstraten leicht an. Durch Anwesenheit von Kaliumchlorid können mehr Nanopartikel produziert werden als in destilliertem Wasser. Diese Nanopartikel, die sich auf der Kupferoberfläche gebildet haben, bestehen aus Kupfer(I)-oxid (Cu_2O) oder Kupfer(II)-hydroxid ($Cu(OH)_2$). Bei einer hohen Spannung und hohen Frequenz ist eine größere Oberflächenstruktur erkennbar. Eine kleine Distanz zwischen Kupferoberfläche und Plasma, sowie der beiden Elektroden zueinander, verbessert die Oberflächenstruktur.

Abstract

In-liquid-plasmas provide versatile applications in chemistry, biomedicine and industry. One possible application is the chemical synthesis and growth of nanoparticles. Copper (Cu) nanoparticles, for example, are used as catalysts in electrochemical conversion of carbon dioxide (CO_2). Properties of catalysts can be altered through the chemical reactions generated by pulsed plasma inside the liquid. The deterioration of the catalytic activity is a major challenge in nowadays electochemical cells. Therefore, pulsed plasmas in liquid may reactivate the Cu nanoparticle catalysts on the Cu surface while being inserted into an electrochemical cell.

In this thesis, the surface structure of plasma treated Cu substrates used in electrochemical cells are analysed. These Cu substrates are treated with nanosecond and microsecond pulsed plasma in liquid by varying plasma parameters like voltage and frequency. Distilled water and a potassium chloride solution at a concentration of 0.0035 M are used as liquid. The plasma treated Cu foils were investigated by scanning electron microscopy and X-ray photoelectron spectroscopy. More nanoparticles can be produced in the presence of potassium chloride (KCl) than in distilled water. These nanoparticles formed on the Cu surface consist of cuprous oxide (Cu_2O) or cupric hydroxide ($Cu(OH)_2$). At a high voltage and high frequency, a larger surface structure change can be observed. With small distances between Cu sample and plasma, as well as with small distances of the electrodes to each other, nanoparticles with a more cubis shape can be synthesized.

Contents

1 Motivation

In industry, plasma discharges are applied for surface modification of materials and surface processing in integrated circuit processing [1], but they also offer versatile applications in chemistry and biomedicine. Biological effects are caused by changes of the liquid environment of the biological systems like proteins, cells and tissue. An application of plasma-liquid interactions for medical purposes is the decontamination of toxic compounds in liquids [2, 3].
If a plasma gets in contact with a liquid, the interaction between plasma and liquid can produce reactive species that react with the compounds in the liquid [4]. The processes in the liquid generated by plasma treatment involve chemical reactions as well as charge transfer [5], material transport and physical reactions [6, 7].
Various in-liquid plasma methods allow the synthesis of noble metals, alloys and metal-oxide nanoparticles [8]. Most reports on nanomaterial synthesis through plasma generation in liquid have been published after 2005 [9]. Nowadays, there is still an interest in this paricular field of plasma physics and chemistry. As plasma-liquid interactions consist of both plasma and liquid, the properites of the synthesized products can be tuned by varying the liquid parameters or plasma parameters [4]. Plasma treatment allows to control the structuring of a surface by creating defects [10], producing nanopores [11] or altering the surface roughness [12]. Plasma treatment can also be used to clean the surface by removing ligands [13] or to activate nanoparticle catalysts for electrochemical conversion of carbon dioxide (CO_2) [14].
Catalysts such as nanoparticles [15–20], nanocubes [21, 22], nanofoams [23] and nanowires [24] show improved catalytic activity or selectivity over bulk materials [25]. The deterioration of the reactivity of catalysts in an electrochemical cell is a big challenge, but certain aspects like the nanostructure and the oxidaton state of the surface can improve the selectivity of the electrochemical reduction of CO_2 to a variety of hydrocarbons and alcohol [14, 26]. In-liquid-plasma methods may help to modify and recover the catalytic surface during operation of the electrochemical cell. However, plasma-liquid interactions including their effect on surface structures have not been fully understood and there is still a lot of ongoing research in this area.
In this thesis, electropolished Cu surfaces are treated with a nanosecond pulsed plasma in various liquids and are investigated, in order to get a better understanding of the influence of the plasma parameters on the Cu surface structure is used. In addition to the nanosecond pulsed plasma, a microsecond pulser is used to investigate the influence of the pulse length of the plasma on the treated Cu surface. While images by a scanning electron microscope (SEM) give information about the surface structure, size and shape of the synthesized nanoparticles, x-ray electron spectroscopy (XPS) is used to gain information about the elements and compounds, accompanied on the surface. As the growth of nanoparticles alters the compounds on the Cu surface, both techniques com-

plement each other and provide the constituents of the nanoparticles. Cuprous oxide nanoparticles (Cu_2O nanoparticles) and cupric hydroxide nanoparticles ($Cu(OH)_2$ nanoparticles) are formed on the Cu surface through the use of in-liquid plasma, which is also referred as plasma electrolysis [27].

2 Theoretical Background

In this section, the theoretical background on pulsed plasmas in liquids and their influence on Cu surfaces is given. It includes the definition of plasma, information about pulsed plasmas in liquids as well as the surface changes through plasma treatment and the corresponding electrochemistry.

2.1 Plasma definition

The term plasma was defined by Irving Langmuir who observed specific oscillations in an ionized gas [28]. Plasma is a quasi-neutral gas, which consists of positive and negative charge carriers and is characterized by the following properties:

a) Quasi-neutrality

b) Debye length

c) Plasmafrequency

Quasi-neutrality occurs when the number of free positive and negative charge carriers is the same globally and locally except for small deviations. The reason for these deviations is the carrier transport. When small potential perturbations occur, the charge carriers are exponentially shielded in the plasma. The shielding length is referred to as the Debye length λ_D and can be calculated by

$$\lambda_D = \sqrt{\frac{\epsilon_0 k_B T_e}{e^2 n_e}} \tag{2.1}$$

with the dielectric constant ϵ_0, the Boltzmann constant k_B, the temperature T_e of electrons, the electron density n_e and the elementary charge e. Due to possible disturbances, the charge carriers also oscillate with the so-called plasma frequency ω_P:

$$\omega_P = \sqrt{\frac{e^2 n_e}{\epsilon_0 m}} \tag{2.2}$$

There m is the effective mass of the electron or ion [29].
Furthermore, three conditions have to be fulfilled, in order define an ideal plasma state [29]:

a) $L \gg \lambda_D$

b) $N_D \gg 1$

c) $\omega_P \cdot \tau \gg 1$

N_D is the number of electrons in a Debye sphere, which has the radius of a Debye length. The mean collision time between the charge carriers is given by τ and L is the dimension of the plasma.

A plasma is classified as either a thermal equilibrium plasma or a non-thermal equlilibrium plasma. A thermal equilibrium plasma is generated by applying electrical power for a long time under conditions that the gas pressure is 5 kPa or more and that the electron and gas temperatures are nearly equal. In comparison to thermal equlibrium plasmas, a characteristic of non-thermal equilibrium plasmas is that its gas temperature is low and its electrons are in a high-energy state [8].
Because discharges in and in contact with liquids are mostly generated in both gas and liquid state and are in a highly non-equilibrium state, plasma-liquid interactions are non-thermal [30].

2.2 Pulsed plasmas in liquids

Figure 2.1 shows typical discharge setups for plasma-liquid interactions. Generally, plasma in liquid generation can be subdivided into three main categories : (a) Direct discharge between two electrodes in liquids, (b) Gas discharge between an electrode and the electrolyte surface, (c) Bubble discharges between two electrodes in liquids [30].

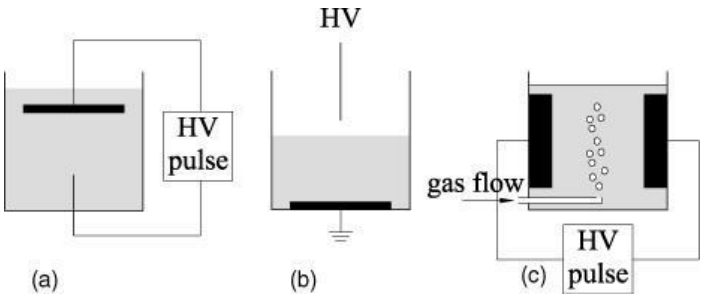

Figure 2.1: Examples for typical electrode configurations: (a) direct liquid phase discharge reactor (b) gas phase discharge reactor with liquid electrode (c) bubble discharge reactor [30].

For further information about electrode configurations, Bruggeman et al. [30] and Saito et al. [31] have presented an overview of various discharge setups for plasma-liquid interaction. Mostly, in-liquid-plasmas are generated in a pin-to-pin or pin-to-plate setup [32–35]. Many researchers have optimized in-liquid-plasmas with regard to factors such as pressure, temperature, density, viscosity, composition and conductivity [36]. Grosse et al. [37] have studied ignition, cavitation and several plasma parameters of nanosecond pulsed plasma in water. Plasma ignition in liquids is assumed to take place in nanopores and causes the generation of a cavitation bubble and pressure waves [37].

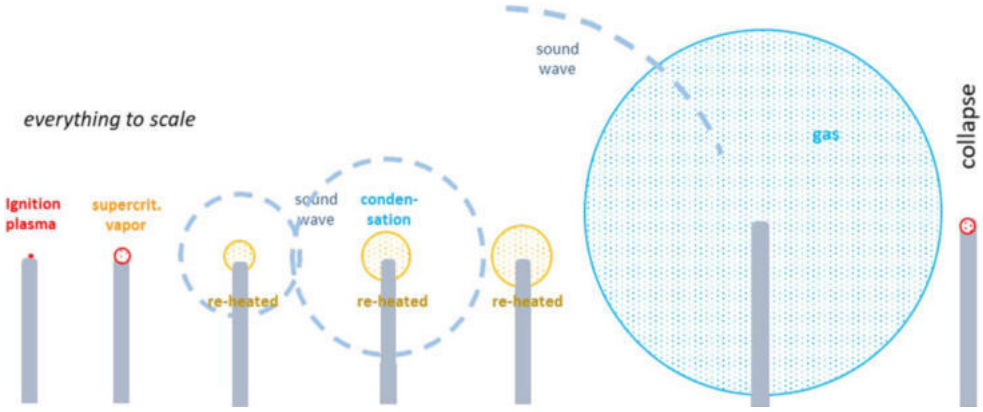

Figure 2.2: Properties after plasma ignition (adopt from [37]).

Figure 2.2 demonstrates the development of an initial supercritical water bubble created by plasma ignition. The reactive species generated by in-liquid-plasma and liquid species couple because of the nature of supercritical water . During expansion of the bubble, the reactive gas condenses and is converted back to the liquid state. The gas inside the bubble is frequently re-ignited by reflected high voltage pulses which oscillate between power supply and discharge chamber [37]. This may lead to further production of reactive species.

2.3 Electrochemistry

In plasma-liquid interactions, chemical and physical processes can be used to synthesize versatile nanoparticles. The synthesis of nanomaterials can be controlled from the solution phase as well as from the plasma phase. For example, the production of reactive species can be tuned by varying the plasma parameters. The created reactive species have different lifetimes and different reducing abilities. Furthermore, various radicals produced by plasma-liquid interactions allow the possibility of controlling the composition and shape of the nanomaterials. This can be achieved by adjusting the plasma parameters [6].
When glow discharges are in contact with water, positively charged ions may represent H_2O^+ species or an ion cluster like for example $H_3O^+(H_2O)_X$ [38–40]. Additionally, the plasma may contain neutral reactive species such as O an OH. These reactive species can interact with species in the liquid [5].
The formation of Cu nanoparticles from plasma-liquid interactions have been studied by Pootawang et al. [41]. An aqueous solution consisting of ascorbic acid, gelatin and $CuCl_2$ is used as liquid. Cu nanoparticles are formed by pulsed plasma generated between two tungsten electrodes in the liquid. Because of the high voltage, electrolysis of water molecules takes place in the plasma zone and hydrogen and oxygen gases are produced. After electrical breakdown for plasma generation, the water molecules become dissociated, ionized and excited. Highly activated radicals and ion species are formed. Pootawang et al. [41] have measured a slight increase in the electrical conductivity of the liquid after plasma

treatment. Thus, the production of reactive species have an impact on the electrical conductivity of the liquid [41].

2.4 Surface changes through plasma

The energy from in-liquid plasmas can be used to drive chemical reactions in the liquid. Thus, nanoparticles of noble metals, alloys and metal-oxid nanomaterials can be synthesized while being in contact with the treated liquid. Horikoshi and Serpone give an overview about the various produced nanoparticles and their in-liquid plasma methods [8].
Plasma treatment is a method to activate nanoparticle catalysts. The removal of capping ligands used in nanoparticle synthesis, the rapid change of the chemical state of the surface at room temperature and the creation of defects or embedded atoms are just some examples used for the improvement of catalytic activity performance by plasma treatment [13, 42–45].
Cu nanocube catalysts, which have Cu(100) facet morphology and ion content of O^{2-} and Cl^{-}, have been designed through plasma treatment by Gao et al. [14]. The electrochemically prepared Cu nanocube samples have been treated with low pressure plasma in a plasma etcher at gas pressure of 400 mTorr of O_2, H_2 and Ar and a power of 20 W for different time periods. The Cu nanocubes have been synthesized electrochemically in aqueous 0.1 M KCl. They have found out that high oxygen content remaining on the nanocube as well as the cubic structure of the Cu nanoparticles are necessary for achieving high catalytic activity. Especially, the presence of surface and subsurface oxygen is essential for the high catalytic activity and ethylene selectivity in CO_2 conversion. While a short exposure of Cu nanocubes to low pressure plasma does not lead to any significant modificaton of the Cu sample morphology, a long exposure to low pressure plasma destroys the Cu nanocubes. Cu nanocubes that have not been treated with plasma have a significant lower oxygen content than those who have undergone plasma treament. Although the O_2 plasma treatment time is smaller than the H_2 and Ar treatment time, O_2 plasma treated Cu nanocube samples retain more oxygen. Part of this oxygen consists of adsorbed species and is not in the form of Cu oxides. Gao et al. [14] gives more detailed information about the plasma-activated Cu nanocube catalysts for CO_2 conversion.

3 Experimental Methods

In this section, the experimental methods are described including electropolishing, plasma treatment and various measurements for surface analysis of Cu substrates.

3.1 Electropolishing of Cu substrates

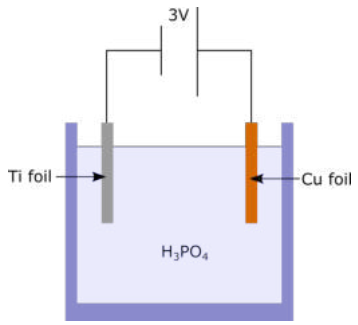

Figure 3.1: Electropolishing of a Cu foil.

The surface roughness of commercial Cu foils can be reduced by electropolishing without mechanical deforming of the Cu surface. Therefore, commercial Cu foils, which have a thickness of 0.1 mm were electropolished before plasma treatment in liquids. For this process, a titanium foil and a Cu foil are dipped in 98 M orthophosphoric acid (H_3PO_4), which is used as an electrolyte. Both foils are faced to each other and are connected with a DC power supply, which provides a voltage of 3 V (Fig. 3.1). After a treatment time of 5 min, the Cu foil is removed from the electrolyte and is cleaned with ultra pure water, in order to remove the orthophosphoric acid.

3.2 Plasma treatment of Cu substrates

Figure 3.2 shows the experimental setup of a discharge chamber, in which electropolished Cu foils are treated with nanosecond pulsed in-liquid-plasma. The plasma can be ignited between two electrodes in the discharge chamber, which is made of polymethylmethacrylat (PMMA) and has a volumetric capacity of 25 ml. The discharge chamber is filled with distilled water or 0.0035 M KCl as liquids.
The top electrode is connected to the commercial high voltage pulse generator FPG 30-01NK10 from FID GmbH, which produces nanosecond pulses of 10 ns width with maximum amplitude of up to 30 kV into 50 Ω load. The electrode contains a Cu rod shielded by a glass tube and is connected to a tungsten wire, which is mounted inside a cannula. The diameter of the tungsten wire is 50 μm. The distance between the grounded bottom electrode and the tip of the tungsten wire varies between 3.7 mm and 6.6 mm depending on the measurement. The electropolished Cu foil is attached with Kapton tape on the sample holder

made of PMMA. Several parameters can be changed for the treament of the Cu substrates, in order to alter the production, size and shape of the nanoparticles. Voltage and frequency can be set on the high voltage pulse generator. The treatment time can be varied. Furtermore, the distance between both electrodes and the distance between sample and tungsten wire can be changed.

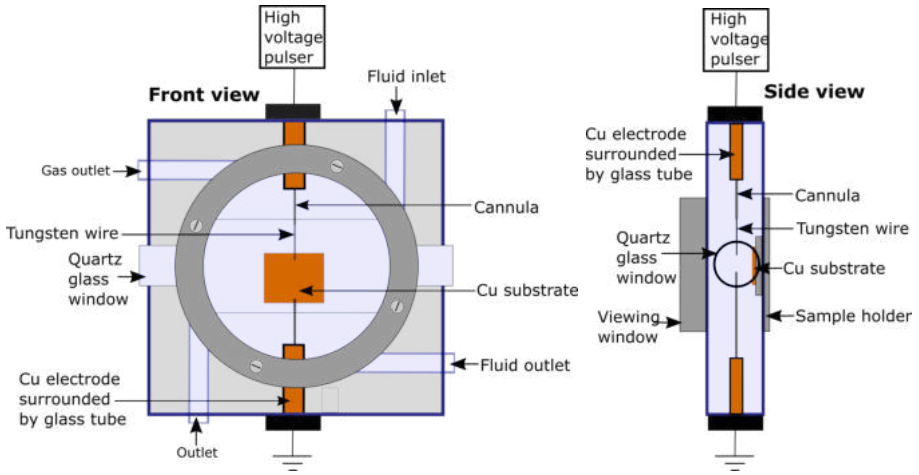

Figure 3.2: Discharge chamber with Cu sample from front view (left) and side view (right).

In 0.1 M KCl as often used in electrochemistry, no nanosecond pulsed plasma can be generated with the presented setup. With a smaller concentration of KCl in the liquid, the conductivity of the solution decreases and a nanosecond pulsed plasma can be ignited in the liquid. Therefore, 0.0035 M KCl is used as a liquid. Due to other pulse properties in comparison to the nanosecond pulsed plasma, the generation of microsecond pulsed plasma in aqueous KCl is tested. However, no plasma can be ignited in 0.1 M KCl. An electropolished Cu foil is therefore treated by a microsecond pulsed plasma in 0.0035 M KCl. The experimental setup of the discharge chamber for microsecond pulsed plasmas is quite similar to that for nanosecond pulsed plasmas. Nevertheless, the cable connections differ from the configuration for the generation of nanosecond pulsed plasmas and the frequency is provided by a function generator. Figure A.3 in the appendix shows the experimental setup of the microsecond pulser. After plasma treatment Cu substrates are stored in a receptacle and are examined with SEM and XPS.

Before and after every plasma treatment the electric conductivity of the liquid is measured with the conductivity meter GLF100 by GHM Messtechnik. The electric conductivity of a liquid depends on the number of charged particles, on their charge and their mobility. The conductivity of distilled water is $(1\pm1)\,\mu\mathrm{Scm}^{-1}$ and the conductivity of 0.0035 M KCl is $(568\pm1)\,\mu\mathrm{Scm}^{-1}$ before plasma treatment.

Furthermore, the distance between both electrodes and the distance between

tungsten wire and sample can be measured by taking images with a camera.

3.3 Surface analysis

The treated Cu surfaces are analysed by using scanning electron microscopy (SEM) and x-ray photoelectron spectroscopy (XPS).

3.3.1 SEM

The Quanta 200 FEG system by the company FEI is used for SEM measurements. The SEM is an instrument for imaging selected areas of solid samples and has a spatial resolution of appoximately 2 nm.

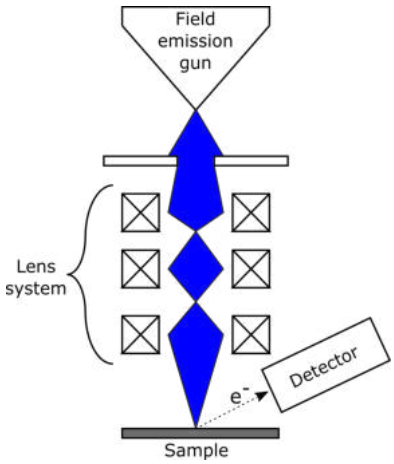

Figure 3.3: Basic construction of SEM.

The basic components of the SEM are the following: field emission gun, lens system, detectors and imaging system (Fig. 3.3). Electrons emitted through the tunnel effect from the field emission gun are accelerated by the anode and emerge from the anode opening. The electron beam enters a lens system, which consists of current-flowing coils surrounded by an iron yoke. The lens system decreases the size of the electron beam and focuses it on the sample. The emitted secondary electrons and back-scattered electrons are detected. For the detection of secondary electrons, the Evehart-Thornley-detector, which contains a scintillator and a photomultiplier, is used, whereas a solid state detector detects the back-scattered electrons. The detected signals are converted to surface images by an imaging system.

3.3.2 XPS

XPS measurements are performed with a PHI5000 X-ray photoelectron spectrometer using a monochromatic Al Kα source, which consists of an Al anode and a quartz crystal monochromator. The XPS is constructed for elemental and chemical analysis of solid surfaces. Chemical information are provided through measurements of the binding energy.

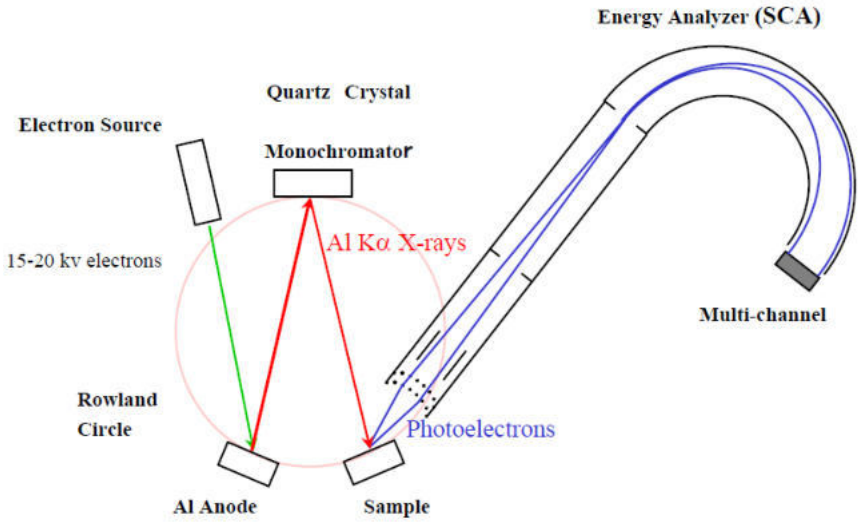

Figure 3.4: Configuration of the focused X-ray source and the energy analyzer [46].

Figure 3.4 images the basic principle of XPS analysis. Monochromatic Al Kα X-rays penetrate into the sample surface and excite photoelectrons. This effect is referred to as photoelectric effect and can be explained by the conservation of energy. The energy of the photon is used in order to overcome the binding energy of the nucleus (Fig. 3.5). The excess kinetic energy of the photoelectrons can be detected by an energy analyzer [46].

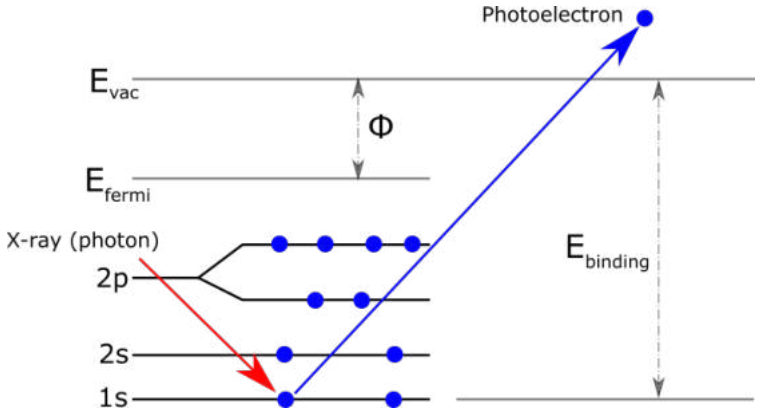

Figure 3.5: Principle of photoelectron excitation (adapted from [46]).

The data obtained are selected areas of the Cu samples. Especially the Cu surface areas close to plasma ignition are examined by recording XPS survey measurements. XPS surveys provide information about the binding energy, which is specific for the elements, the energy levels and the states in which the elements are. The binding energy can be calculated with the following equation:

$$E_{binding} = E_{photon} - E_{kin} - \Phi \tag{3.1}$$

E_{kin} describes the kinetic energy of the photoelectron, E_{photon} is the energy of the photon and Φ is the work function (Fig. 3.5). The photon energy from the Al Kα source is 1486.7 eV [47].
Thus, XPS survey spectra can help to identify the elemental composition of solid surfaces. High resolution measurements are done for some Cu samples, in order to specify the plasma treated Cu surface compounds and to get information about the constituents of the synthesized nanomaterial. In comparison to XPS surveys, XPS high resolution spectra are created by setting small energy steps in the range of 0.005 eV. In addition to photoelectrons, the XPS system can detect Auger electrons. Due to overlapping binding energies for Cu(0) and Cu(I) species in Cu $2p_{3/2}$ XPS spectra, Cu Auger LMM XPS spectra of Cu samples are taken. Charge compensation is carried out with a neutralizer.
When an electron is removed due to a photon and leaves a vacancy, an electron from a higher energy level E_M can fall into the vacancy. The released energy $E_L - E_M$ can be transferred to another electron and causes an ejection from the atom. The ejected electron is called as Auger electron and has a specific kinetic energy E_{kin}, which can be calculated by

$$E_{kin} = E_L - E_M - E_M. \tag{3.2}$$

The kinetic energy of the Auger electron does not depend on the energy of the photon [48].

4 Results and Discussion

As mentioned in section 3.2, this work deals with the synthesis of nanoparticles as well as with the plasma parameters that are necessary for the formation of nanoparticles. For this purpose, various parameter variations are carried out and the occurence of nanocubes is checked by SEM.
First the surface of the Cu samples plasma treated in distilled water is analysed. Then the surface of the Cu samples plasma treated in 0.0035 M KCl is examined. Furthermore, a chemical analysis of the Cu surface will be presented and the compounds of the nanoparticle are discussed and compared with results of another research group.

4.1 Surface analysis of Cu samples treated by plasma in distilled water

In Figure 4.1 electropolished Cu foils after 20 min of plasma treatment in distilled water are presented. Thereby, the frequency of the nanosecond pulser is 15 Hz and the voltages vary between 20 kV and 26 kV depending on the treated Cu foil. The electropolished Cu foils have a smooth surface before plasma treatment. After plasma treatment, there are no significant surface structure observed by SEM on the surface areas close to plasma ignition. Only at voltages higher than 24 kV nanoparticles are formed. The created nanoparticles seem to have a round shape and a particle size of approximately 50 nm.
Spherical aberration, chromatic abberation, diffraction error and astigmatism lead to image errors, whose effect is noticeable at high magnifications. Therefore, no cubic structure of the nanoparticels can be observed. By applying a high voltage, more power goes into the generated plasma. Thus, more chemical reactions take place in the distilled water and versatile reactive species are produced. Previous investigations of plasma-liquid interactions show that hydrogen peroxide (H_2O_2) is produced, among other species [49]. The created reactive species may react with the Cu surface and form nanoparticles. With more power going into the discharge, the amount of the created particles inside the distilled water is higher.
Figure A.1 in appendix shows Cu surfaces treated by nanosecond pulsed plasma in distilled water. The plasma treatment time is 20 min. The frequency varies between 15 Hz and 30 Hz, while a voltage of 20 kV is applied. A higher frequency at the power supply system leads to no significant surface structure change on the area close to the electrode tip. The Cu surface areas do not differ radically from the electropolished Cu substrate and are still smooth and shiny after plasma treatment in distilled water. Applying a high frequency increases the average power that goes into the plasma. The created reactive species may have not enough energy to react with the Cu surface despite of the higher average power. Presumambly, a certain voltage must be applied, in order to generate enough reactive species that can interact with the Cu surface.

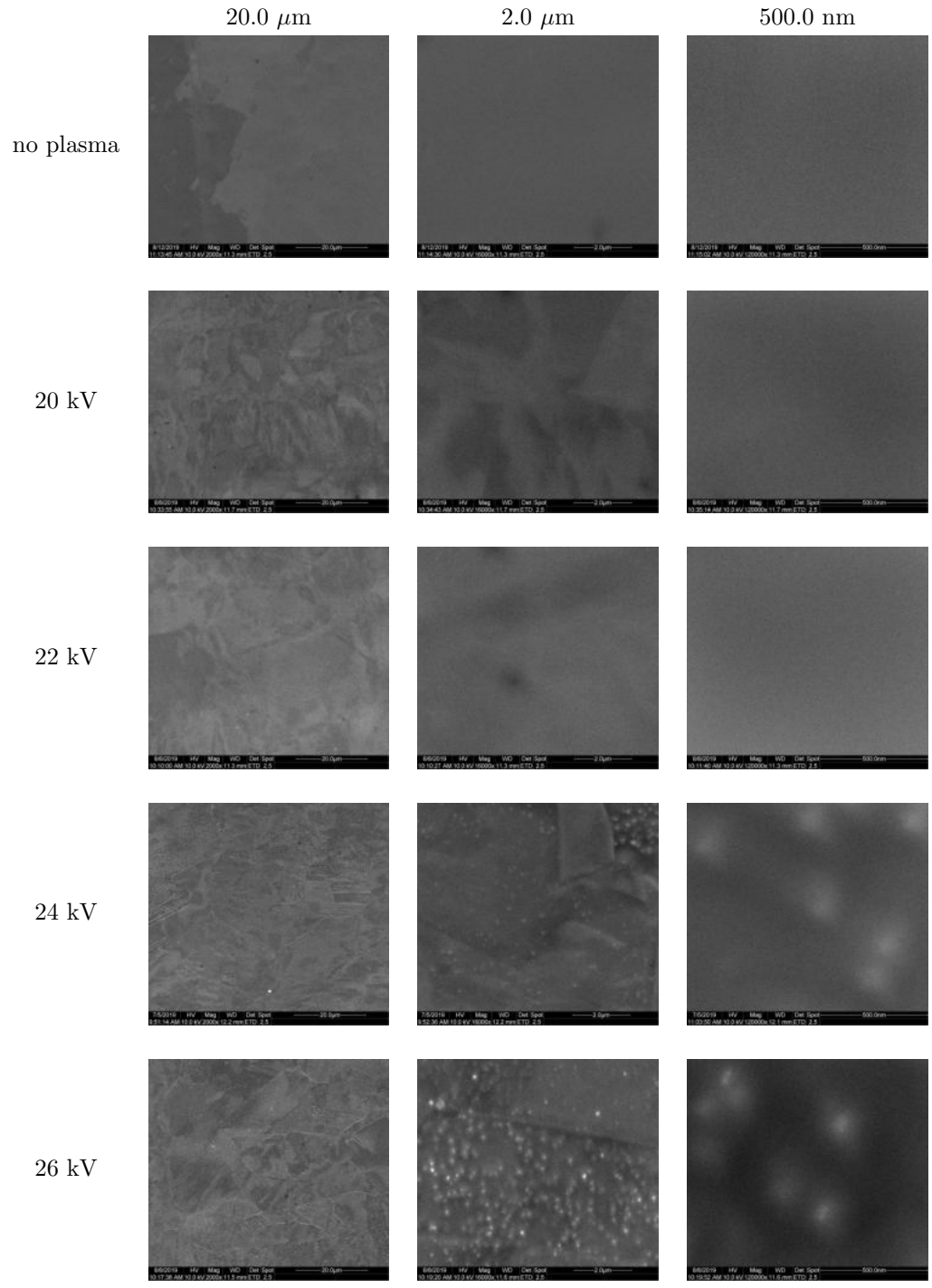

Figure 4.1: Voltage variation: Electropolished Cu foils after 20 min of plasma treatment in distilled water are shown. The frequency of the nanosecond pulser is 15 Hz and on the left side the voltage of the nanosecond pulser is given. The distance between both electrodes is (3,7±0,9) mm and the distance between Cu sample and tungsten wire is (2,9±0,7) mm. Before plasma treatment water conductivity of 1 μScm^{-1} is measured. Only areas close to the plasma ignition are shown. The labels above the column indicate the size of the image.

In comparison to Figure A.1, Figure 4.2 shows the variation of electrode distance for a voltage of 20 kV, a frequency of 15 Hz and a plasma treatment time of 20 min inside distilled water. A small distance between both electrodes can increase the generated electric field E according to $E = -\frac{U}{d}$ with U being the applied voltage and d the electrode distance. This has an impact on the properties of the in-liquid-plasma and causes various chemical reactions. Thus, an increase in the electric field may lead to more reactive species. Nevertheless, no significant surface structure change on the area close to plasma is given in comparison to an only electropolished Cu foil. However, in little areas of the Cu foil nanoparticles can be found. At smaller distances between both electrodes, more cubic shaped nanoparticles can be observed (Fig. 4.2).

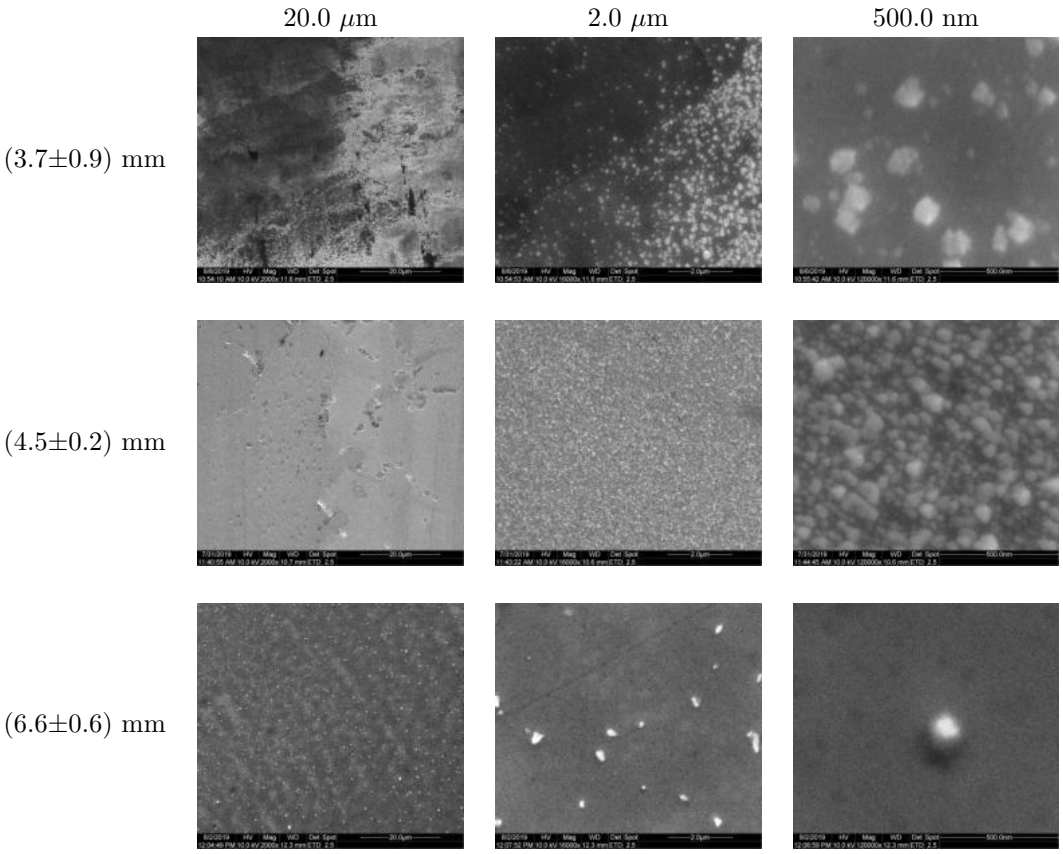

Figure 4.2: Various distances between both electrodes: Electropolished Cu foils after 20 min nanosecond pulsed plasma treatment in distilled water are shown. A voltage of 20 kV and a frequency of 15 Hz are applied. Before plasma treatment water conductivity of 1 μScm^{-1} is measured. On the left side the distances between both electrodes are given and the labels above the column indicate the size of the image. Only areas where nanoparticles have been found are shown.

In comparison to Figure 4.2, Figure 4.3 shows the variation of the distance between sample and tungsten wire. Other plasma parameters like freqeuncy and voltage of the pulser remain constant. A voltage of 16 kV and a frequency of 15 Hz is applied. The plasma treatment takes 20 min. the Cu surface areas treated with nanosecond pulsed plasma in distilled water. The distance between sample and tungsten wire is varied, while other parameters like frequency and voltage of the pulser as well as the treatment time remain constant. On surface areas close to plasma ignition no nanoparticle can be found. Only on some small areas of the Cu surface, nanoparticles have been observed. At a distance of (3.9±0.3) mm between sample and electrode nanoparticles with a more cubic shape can be produced in comparison to the sample with a distance of (6.9±0.3) mm between sample and electrode, although it is operated at a voltage of 16 kV.

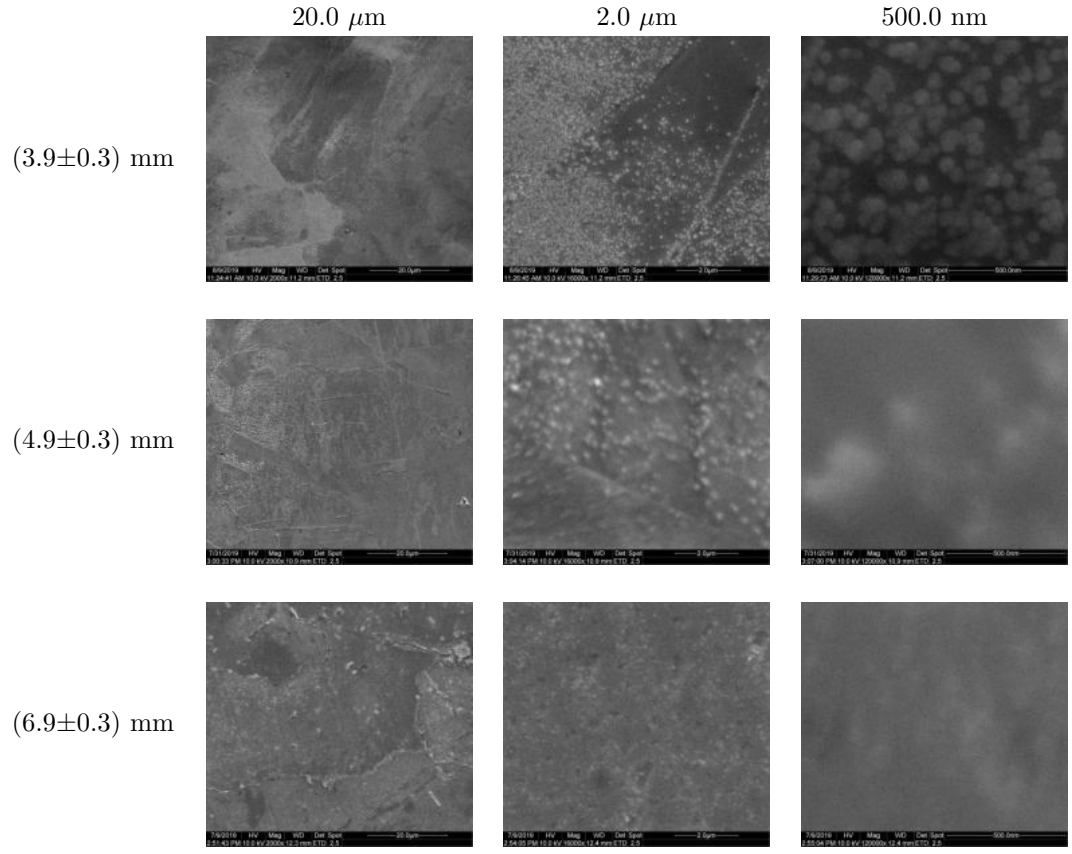

Figure 4.3: Various distances between sample and electrode: Electropolished Cu foils after 20 min plasma treatment in distilled water are presented. A voltage of 16 kV and a frequency of 15 Hz are applied. Only areas, where nanoparticles have been found, are shown. On the left side the distance between tungsten wire and Cu sample is given and the labels above indicate the size of the image.

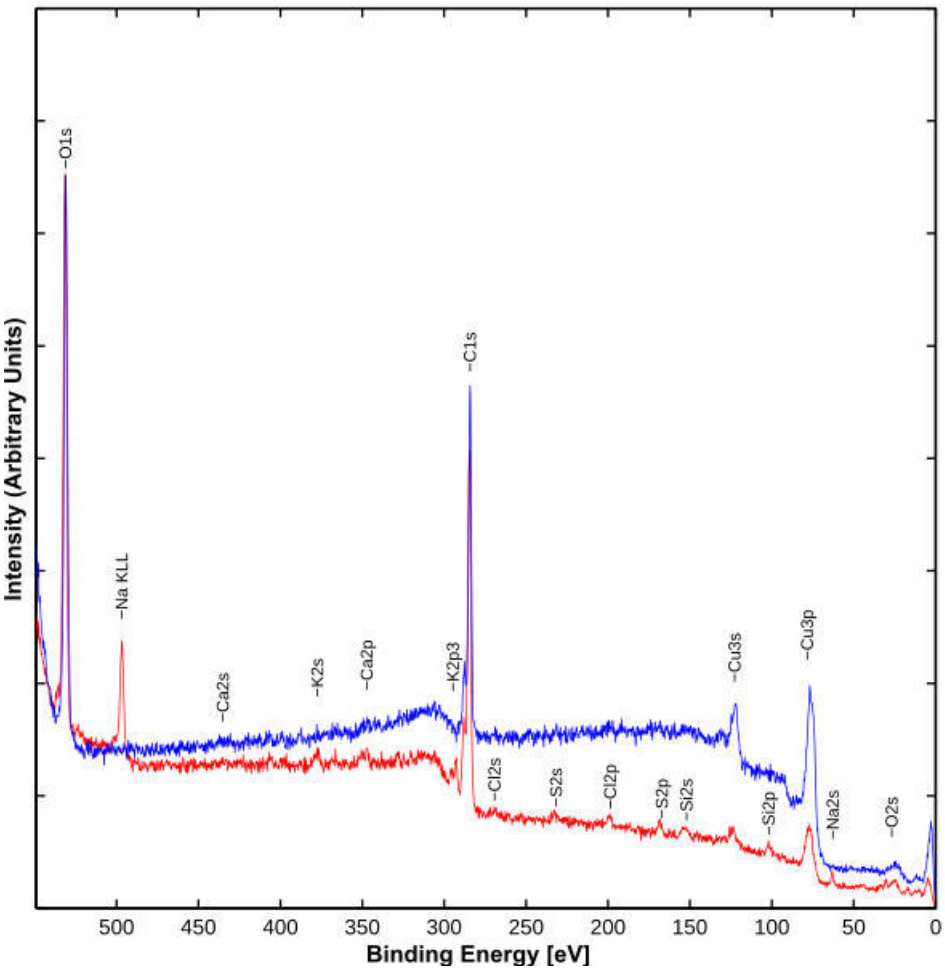

Figure 4.4: XPS survey of a Cu sample treated in distilled water. The voltage of the nanosecond pulser is 20 kV and the frequency is 15Hz. The treatment time is 20 min. The blue curve is related to an area close to nanosecond plasma where no nanoparticles have been found. The red curve shows a selected area where nanoparticles have been found.

On most Cu samples treated in distilled water no or only a few nanoparticles have been found - especially, in the area close to plasma ignition. The Cu surfaces seem to be smooth and shiny there. Just some small areas of the Cu surfaces are changed significantly in comparison to an untreated electropolished Cu foil. In Figure 4.4 the XPS survey spectra of two areas of the same Cu surface are presented as an example for plasma treated Cu substrates in distilled water. The area close to plasma ignition shows no nanoparticles under the SEM. Only on a small area the surface structure is changed. Due to the oxidation of this small area through the chemical reactions generated by plasma, the surface area changed its colour to a more orange one compared with the remaining surface. After examining the area with SEM it has been found out that there are nanoparticles. The XPS survey spectra show that on the areas, where nanoparticles are found, there are elements like potassium (K), chloride (Cl), sodium (Na) and silicon (Si) (red curve in Fig. 4.4). Presumambly, salts like

potassium chloride (KCl) have been in the corners of the discharge chamber, which may lead to the contamination of the distilled water. By examining the elements of kapton tape, which is used to fix the Cu substrate on the sample holder, it has been found out that Kapton tape contains Si. Instead of using Kapton tape for the fixing of the Cu substrates, a new sample holder is designed which does not require Kapton tape in order to avoid the contaminations which possibly arise from the tape (Fig. A.4).
The presence of salts may have an impact on the production of nanoparticles and the nanoparticles have been synthesized due to the contamination of the discharge chamber. Furthermore, aqueous KCl is part of the electrolyte in electrochemical cells. Therefore, Cu samples which are treated with a plasma in aqueous KCl are examined.

4.2 Surface analysis of Cu samples treated by plasma in 0.0035 M KCl

First, the electropolished Cu samples have been put into 0.0035 M KCl without plasma treatment and have been analysed by using SEM, in order to detect any changes on the Cu surface. Figure A.2 in appendix shows that even after 2 min injection time without plasma treatment nanoparticles are formed on the Cu surface. After 5min crosslike strucures are build. After 20 min injection time the layer seem to be thicker than after 2 min. The size of particles vary between 50 nm and 2 μm.
When nanoparticles are created by plasma treatment in 0.0035 M KCl, the size of nanoparticles seem to be smaller than the nanoparticles that have been created without plasma. The nanoparticles that have been synthesized without plasma treatment seem to be more agglomerated on the Cu surface in comparison to the plasma treated Cu nanoparticles (Fig. 4.5). In Figure 4.5 the nanosecond pulsed plasma treated Cu surface areas close to plasma ignition are shown. These Cu substrates are treated in 0.0035 M KCl after electropolishing. By varying the voltage on the high voltage pulser, the plasma power can be altered and the production of reactive species changes. The interaction between the reactive species and the Cu surface may influence the production of surface nanoparticles. At a voltage of 20 kV the size of the nanoparticles varies between 20 nm and 60 nm. At a voltage of 24 kV the size of the nanoparticles varies between 20 nm and 110 nm. However, the oxide layer seem to be thicker at higher voltages, although no systematic trend can be identified. In Figure 4.6 Cu surface areas close to the electrode tip and treated in 0.0035 M KCl are shown. The frequency is varied between 15 Hz and 30 Hz. At higher frequencies the oxide layer seem to be thicker and the nanoparticles seem to have a more cubic shape. The most nanoparticles have been produced at a voltage of 30 Hz in the local area. However, further investigations are required in order to make a clear statement about the impact of the voltage variation and the frequency variation on the Cu surface.

By generating a plasma in the liquid, further versatile reactive species can be produced. These species can react with the copper surface and probably reduce the agglomeration of the nanoparticles. Thus, the nanoparticles on the plasma treated Cu surface seem to be less agglomerated and smaller compared to the Cu samples which are treated in aqueous KCl without plasma treatment. The growth of nanoparticles is dependent on the surface reaction and the diffusion of monomers to the surface [50].

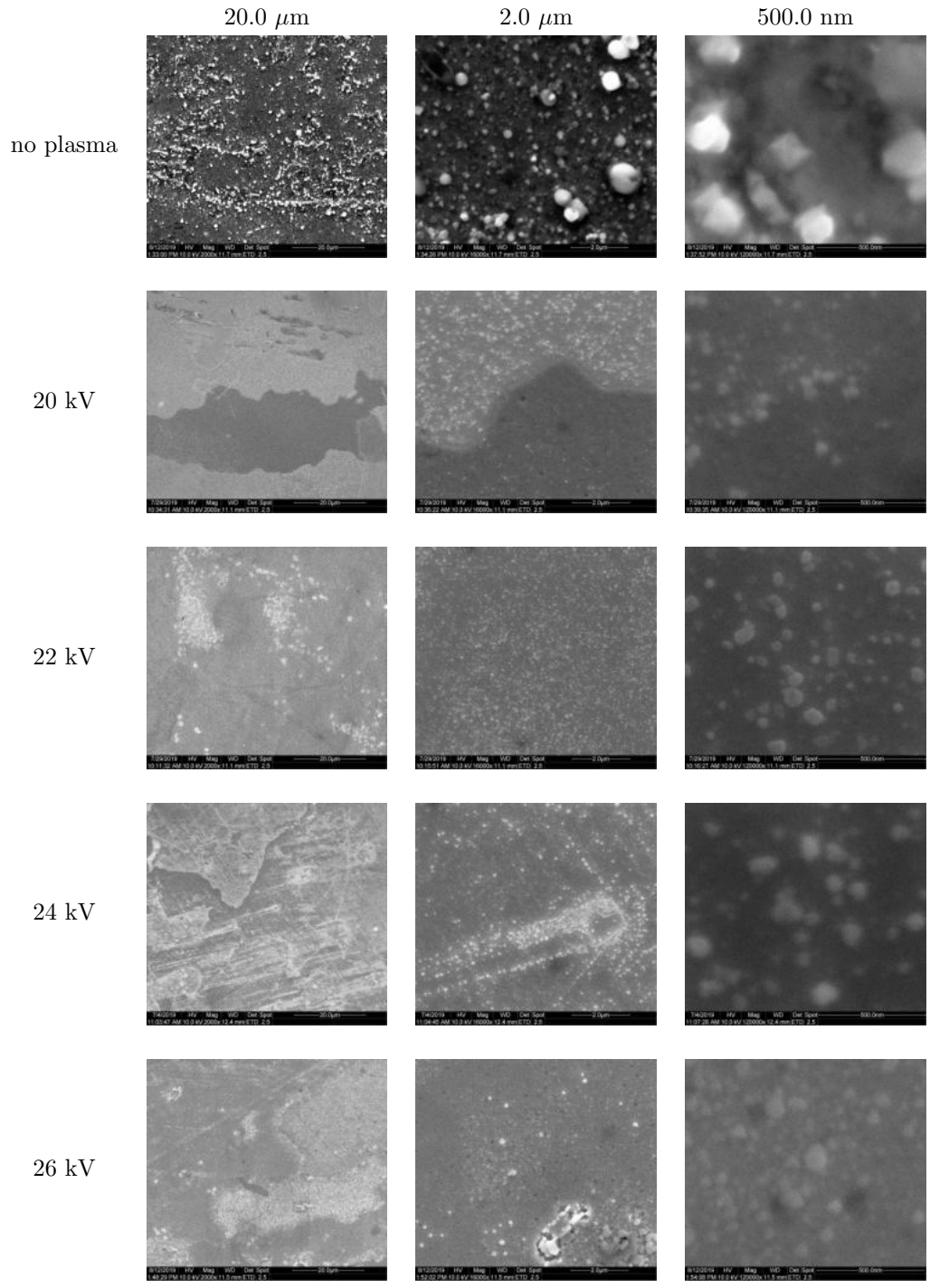

Figure 4.5: Voltage variation: Electropolished Cu foils after 20 min plasma treatment in 0.0035 M KCl are presented. The nanosecond pulser is set to 15 Hz, while the voltage varies from 20 kV to 26 kV. Before plasma treatment the liquid conductivity is 568 μScm^{-1}. Only areas close to the plasma ignition are shown. The labels above the column indicate the size of the image and the voltage is given on the left side.

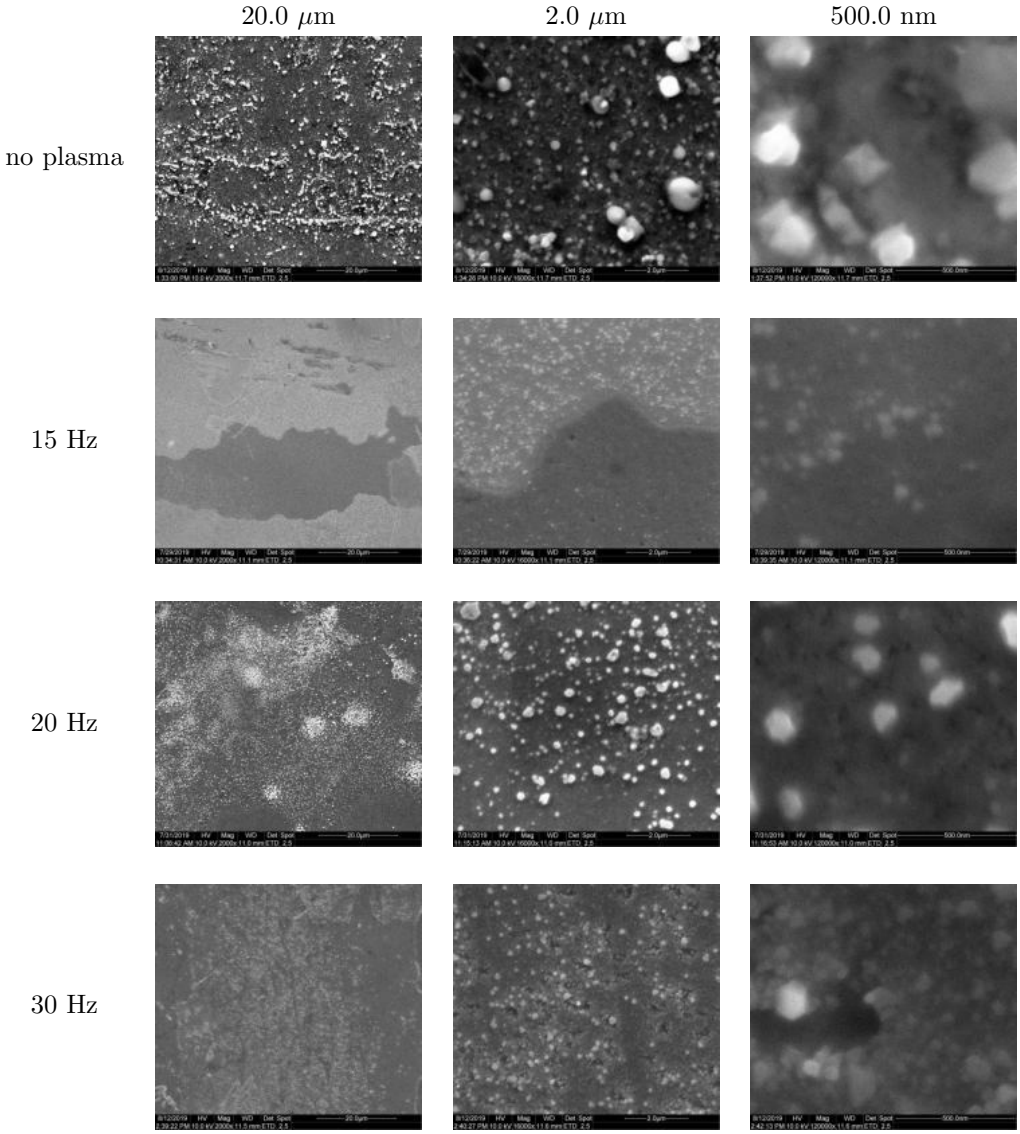

Figure 4.6: Frequency variation: Electropolished Cu foils after 20 min plasma treatment in 0.0035 M KCl are presented. The voltage of the nanosecond pulser is 20 kV and frequency is given on the left side. Before plasma treatment the liquid conductivity is 568 μScm^{-1}. Only areas close to the plasma ignition are shown. The labels above the column indicate the size of the image.

4.3 Chemical analysis of Cu samples

Marked positions of various Cu surfaces are analysed with SEM and XPS, in order to examine the compounds of the nanoparticles. The binding energies for Cu metal and Cu(I) species are overlapped in Cu $2p_{3/2}$ XPS spectra and because of that it is quite challenging to analyse Cu species [51]. Therefore, Cu Auger LMM XPS spectra of Cu samples are taken (Fig. 4.7 - 4.11). Instead of using deconvolution for XPS spectra analysis, the XPS high resolution spectra are examined by comparing the measured peaks with the Cu LMM Auger peak maxima of various compounds given by Biesinger et al. [51]. A high measured peak that concurs with a literature given Cu LMM Auger peak maximum indicates an amount of this specific compound.

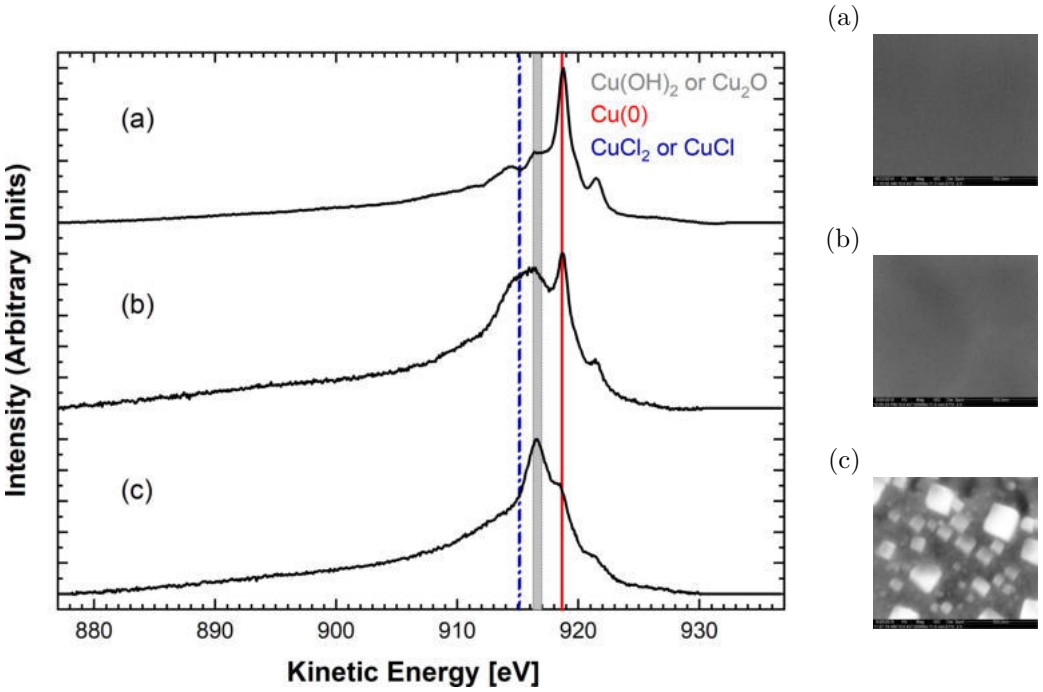

Figure 4.7: XPS high resolution spectra and SEM images that have a scale bar of 500.0 nm: (a) Electropolished Cu surface without plasma treatment, nanosecond pulsed plasma treated Cu surface area in distilled water (b) close to plasma ignition and (c) where nanocubes have been found. A voltage of 16 kV and a frequency of 15 Hz are applied. The plasma treatment time is 20 min.

In Figure 4.7 XPS high resolution spectra and SEM images of the related Cu surface areas are presented. Electropolished Cu foils have a smooth surface with no nanoparticles (Fig. 4.7a). The XPS high resolution spectrum of the untreated Cu surface is very similar to the Cu LMM spectrum for Cu(0) published by Biesinger et al. [51]. Thus, the surface of an untreated Cu sample contains Cu(0). When these Cu foils are treated with plasma in distilled water, Cu on the sample surface oxidizes. In Figure 4.7b the second highest peak of

the XPS spectrum is higher than that of an untreated electropolished Cu sample. This peak could indicate the presence of Cu_2O or $Cu(OH)_2$ on the plasma treated Cu sample. Indeed, there is a stronger oxidation in the area close to the ignited plasma (Fig. 4.7b) compared to the untreated Cu surface. On another area of the same Cu sample, nanoparticles are formed (Fig. 4.7c). These nanoparticles have a cubic form and are hence called nanocubes. The related XPS high resolution spectrum seems to be a mixture of a Cu LMM spectrum of Cu_2O, $Cu(OH)_2$ and Cu(0). Thus, the nanocubes may consist of Cu_2O or $Cu(OH)_2$. Unfortunately, this Cu sample is not reproducible despite same conditions. In spite of using distilled water, elements like sodium, potassium and chloride are measured on the treated Cu surface, but only in the area where also nanoparticles are found. Presumably, the Cu sample was not properly cleaned beforehand. It is possible that salts like NaCl and KCl have been in the corners of the discharge chamber. This contamination could have led to the synthesis of nanocubes. Gao et al.[14] have also produced Cu nanocubes by electrochemically anodizing Cu foils in aqueous 0.1 M KCl with triangular potential scans *vs.* reversible hydrogen electrode. The production of nanocubes may be dependent on the content of KCl in the liquid. According to the surface analysis, more nanoparticles can be produced in the presence of KCl.

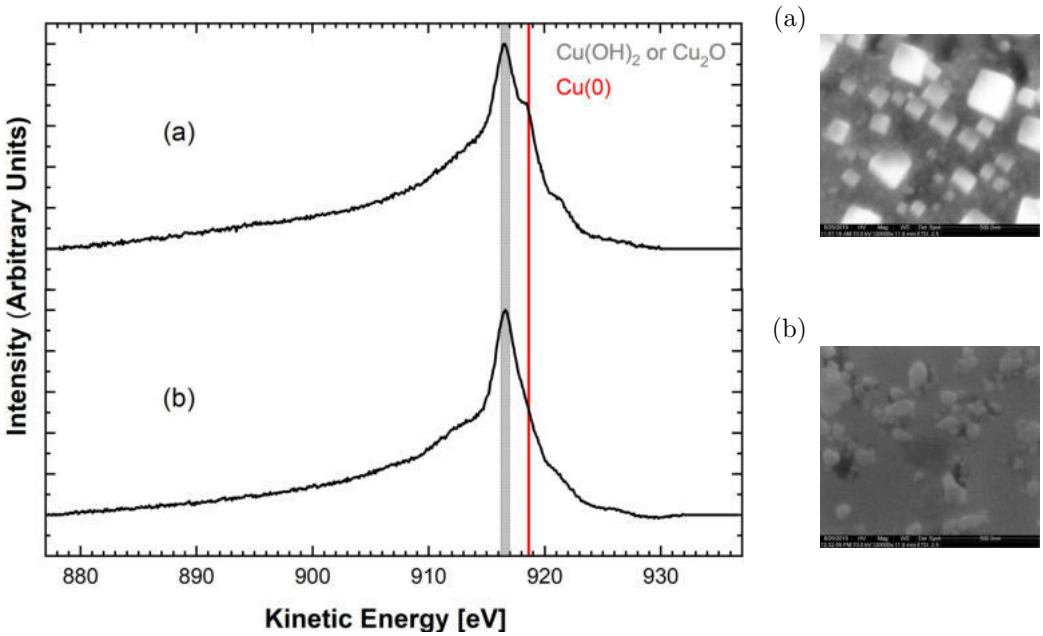

Figure 4.8: XPS high resolution spectra and SEM images that have a scale bar of 500.0 nm: Nanosecond pulsed plasma treated Cu surface area close to plasma ignition (a) in distilled water and (b) in 0.0035 M KCl. For the plasma treatment in distilled water 15 Hz and 16 kV are applied and for the plasma treatment in 0.0035 M KCl 15 Hz and 20 kV are applied. Both Cu samples are treated for 20 min.

If electropolished Cu foils are treated with plasma in 0.0035 M KCl, the surface

structure of the whole Cu sample changes and nanoparticles can be observed on almost every area of the Cu surface. Less Cu metal is measured on the area of the Cu sample treated with KCl (Fig.4.8). Probably more Cu_2O or $Cu(OH)_2$ can be produced with plasma treatment in KCl.

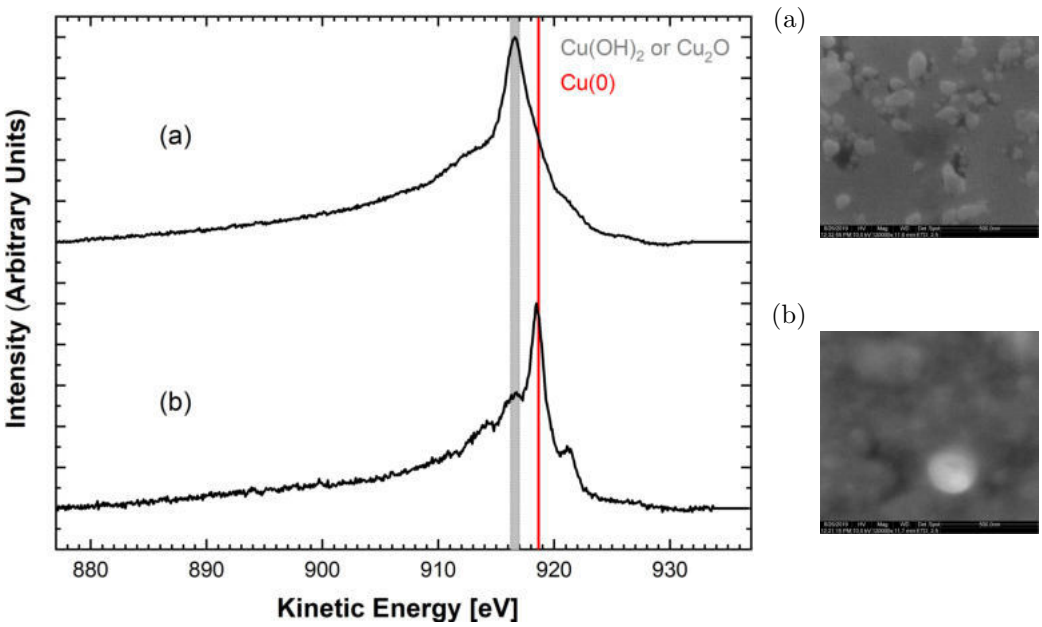

Figure 4.9: XPS high resolution spectra and SEM images that have a scale bar of 500.0 nm: Nanosecond pulsed plasma treated Cu surface area in 0.0035 M KCl (a) close to plasma ignition and (b) further away. The Cu sample is treated for 20min. A frequency of 15 Hz and a voltage of 20 kV are applied.

By comparing the results of the Cu sample treated with KCl with another area of the same sample, more Cu metal is shown in the XPS spectrum (Fig.4.9). The size and the density of the nanoparticles is related to the position on the Cu sample and depends probably on the distance of the ignited plasma to the sample surface area. When the distance between sample surface area and plasma is larger in comparison to other areas, then the surface area seems to be less oxidized and the nanoparticles are smaller.

If the electropolished Cu sample is put into 0.0035 M KCl solution, the Cu surface structure changes and particles have formed even if no plasma has been generated. In addition to this, it can be observed that in the area with a higher density of nanoparticles there is a larger oxidaton on the surface. However, there is still a recognizable difference in the morphology between this sample and the sample treated with plasma. Without plasma treatment the particles seem to accumulate in groups and are more agglomerated than the nanoparticles on the plasma treated Cu surfaces.

Instead of a nanosecond voltage pulser, a microsecond voltage pulser is used to treat the Cu sample in 0.0035 M KCl. A voltage of 24 kV and a frequency of 15 kHz are set on the microsecond pulser. The plasma treatment time is 20 min.

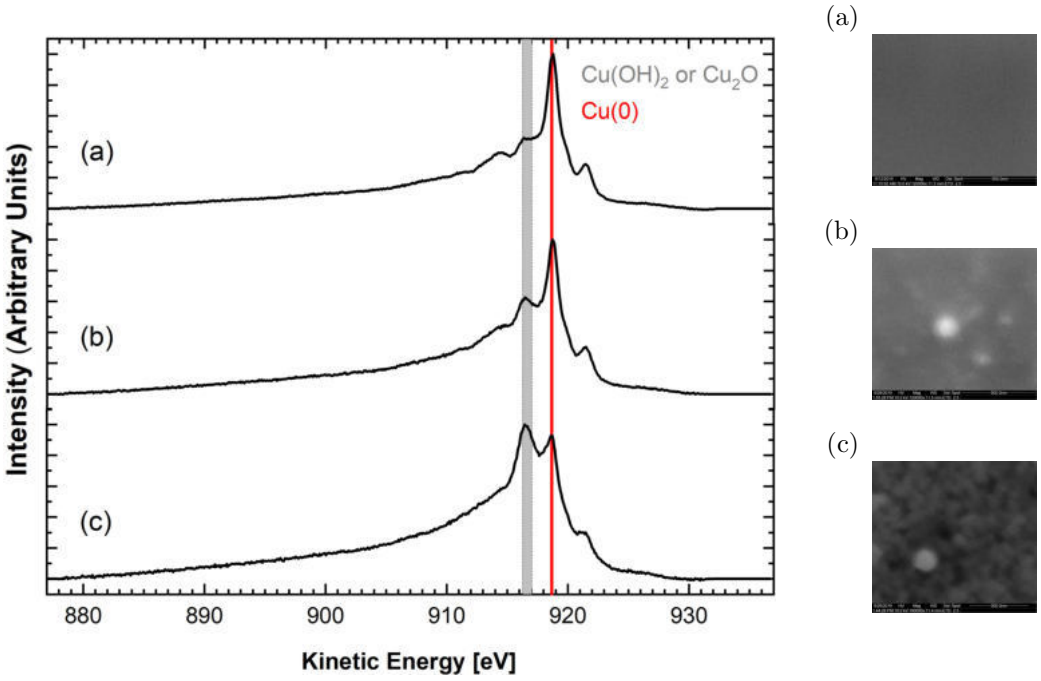

Figure 4.10: XPS high resolution spectra and SEM images that have a scale bar of 500.0 nm: (a) Electropolished Cu surface and (b)-(c) Cu surface areas treated in 0.0035 M KCl without generation of in-liquid-plasma.

Compared to the nanosecond pulsed plasma treated Cu sample, the nanoparticles seem to have a higher density. The nanoparticles on both Cu samples seem to have approximately similar sizes, but the morphology is different. On the microsecond plasma treated Cu sample so called cornfield structures can be observed under the SEM.

Figure 4.12 describes the fraction of oxygen in copper on various Cu samples. On the areas of the Cu samples, where many nanoparticles have been found, the fraction of oxygen in copper is larger.

To summarize, the nanoparticles are formed on plasma treated Cu surfaces in 0.0035 M KCl and consist of Cu_2O or $Cu(OH)_2$. However, nanoparticles are also formed on the Cu surface in aqueous KCl without plasma treatment. Because more nanoparticles are formed in the presence of KCl than in distilled water, KCl seem to be an important compound for nanoparticle formation. Electrochemical reactions at solid-liquid interfaces can be classified into two classes: oxidation and reduction . While cathodic processes involve the reduction of positively charged ions, anodic processes are characterized by the release of electrons from the electrode and oxidation of a species in the electrolyte [5]. Similar to chlor-alkali electrolysis [52], Chlorine (Cl_2) and hydrogen gas (H_2) may be produced in aqueous KCl

$$2KCl + 2H_2O \longrightarrow 2KOH + Cl_2 + H_2 \tag{4.1}$$

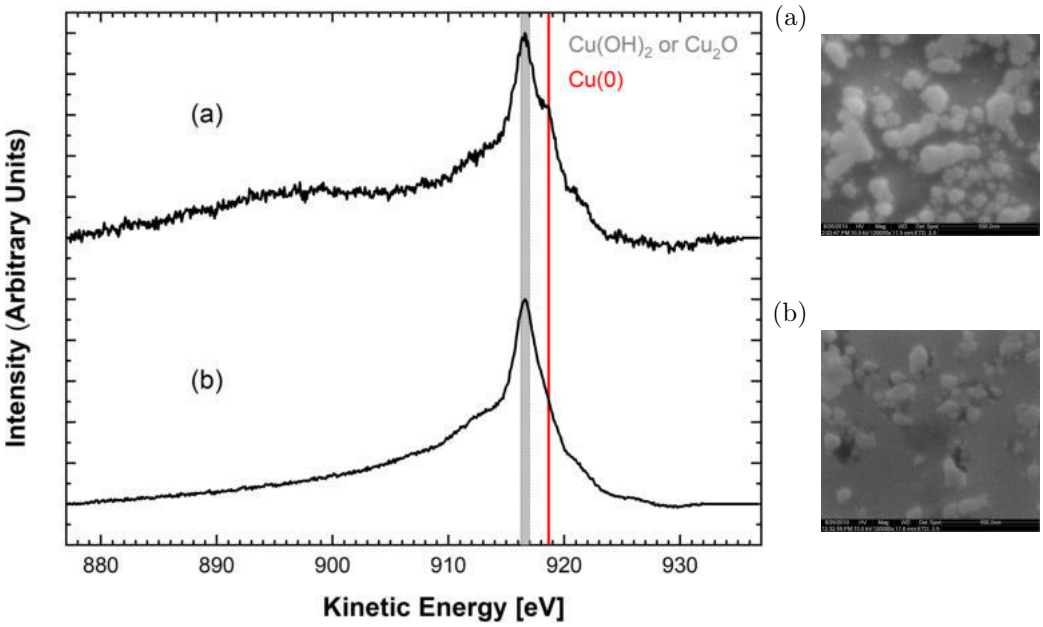

Figure 4.11: XPS high resolution spectra and SEM images that have a scale bar of 500.0 nm: (a) Microsecond and (b) nanosecond pulsed plasma treated Cu surface areas close to plasma ignition. While a voltage of 20 kV and a frequency of 15 Hz are set on the nanosecond pulser, 24 kV and 15 kHz are set on the microsecond pulser. Both Cu samples are treated for 20 min.

The production of potassium hydroxides (KOH) have an impact on the pH of the liquid. Saito et al. [53] have found out that the phase of the synthesized nanomaterial is controlled by the pH of the liquid. Cu on the Cu sample surface may oxidize, while hydrogen ions may be reduced:

$$\mathrm{Cu} \longrightarrow \mathrm{Cu}^{2+} + 2e^- \tag{4.2}$$

$$2\mathrm{H}^+ + 2e^- \longrightarrow \mathrm{H}_2. \tag{4.3}$$

Thus, copper(II) chloride (CuCl_2) can be formed through the chemical reaction

$$\mathrm{Cu} + \mathrm{H_2O} + 2\mathrm{KCl} \longrightarrow \mathrm{CuCl_2} + \mathrm{H_2} + 2\mathrm{KOH} \tag{4.4}$$

KOH or $\mathrm{H_2O}$ may react with $\mathrm{CuCl_2}$ and form copper(II) hydroxide.

$$2\mathrm{KOH} + \mathrm{CuCl_2} \longrightarrow 2\mathrm{KCl} + \mathrm{Cu(OH)_2} \tag{4.5}$$

$$2\mathrm{H_2O} + \mathrm{CuCl_2} \longrightarrow 2\mathrm{HCl} + \mathrm{Cu(OH)_2} \tag{4.6}$$

Cupric hydroxide According to the previous reactions, the synthesized nanoparticles would only consist of $\mathrm{Cu(OH)_2}$. However, the areas of the Cu samples where nanoparticles can be observed are more orange coloured. This may indicate the synthesis of $\mathrm{Cu_2O}$ which can appear either yellow or red [54]. The reduction of Cu^{2+} to Cu^{+} with free radicals in the liquid can result in $\mathrm{Cu_2O}$

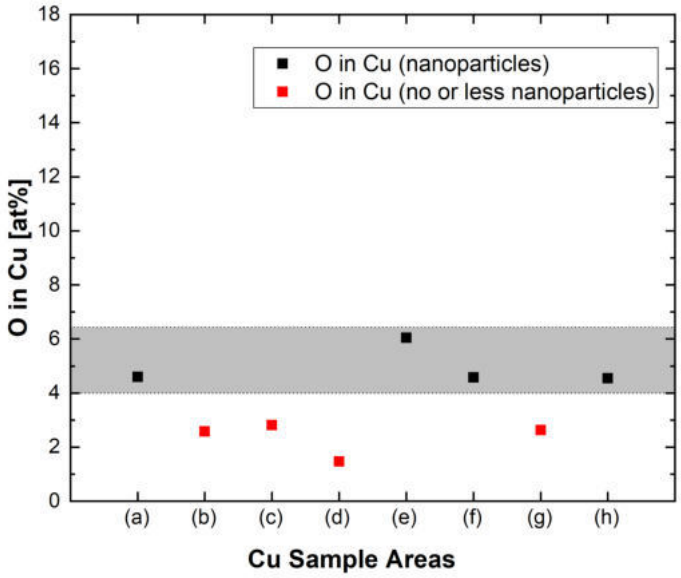

Figure 4.12: Overview on oxygen-in-copper content of various Cu surface areas: (a)-(b) Nanosecond pulsed plasma treated Cu surface areas in distilled water, (c) electropolished Cu surface, (d)-(e) nanosecond and (f) microsecond pulsed plasma treated Cu surface areas in 0.0035 M KCl, (g)-(h) Cu surface areas treated in 0.0035 M KCl

precipitate as the final product [55]:

$$Cu^{2+} + e^{-} \longrightarrow Cu^{+} \tag{4.7}$$

$$Cu^{+} + H_2O \longrightarrow CuOH + H^{+} \tag{4.8}$$

$$2CuOH \longrightarrow Cu_2O + H_2O \tag{4.9}$$

$$2Cu^{+} \leftrightarrow Cu^{2+} + Cu \tag{4.10}$$

Due to the reaction of $2Cu^{+}$ to Cu^{2+} and Cu, the lifetime of Cu^{+} is short [55]. Because versatile reactive species can be produced in plasma-liquid interfaces, it is challenging to find out about the chemical reactions in the liquid and on sample surface. The above mentioned reactions are examples for the chemical reactions that might have happened, but other reactions are not excluded. Further investigations of the plasma-liquid interface as well as of the solid-liquid interface are needed.

5 Conclusion and Outlook

Untreated and plasma treated Cu foils inside distilled water and 0.0035 M KCl solution are invesitgated by SEM and XPS analysis. For Cu substrates treated with plasma in distilled water either no or only few nanparticles can be found, depending on the applied voltage. For voltages above 24 kV the plasma treated Cu sample show sporadic nanoparticle formation on the surface. The synthesized nanoparticles may consist of Cu_2O or $Cu(OH)_2$. More nanoparticles can be produced through the electrochemical reaction generated by nanosecond pulsed plasma in aqueous 0.0035 M KCl. The presence of KCl seems to have an impact on the production rate of nanoparticles. A long exposure of Cu samples to aqueous KCl leads to a thicker nanoparticle layer and a larger change in the morphology. At high voltages and high frequencies of the nanosecond plasma, a larger surface roughness of plasma treated Cu samples can be achieved. However, no clear, systematic and controlled organization of the nanoparticles on the whole Cu surface have been found. Small distances between plasma location and Cu sample help to create nanoparticles with a more cubic shape and to get a rougher surface in the areas, where nanoparicles have been produced. Nanocubes are catalyst with a higher catalytic activity than nanoparticles with a round shape. Thus, it may be more effective to work with small distances between sample and plasma location for designing of cubic catalysts.
Additionaly, a new sample holder for the discharge chamber is designed, in order to fix the sample on the sample holder without using kapton tape. On this way, silicium does not get in contact with the Cu sample in the discharge chamber and the contamination on the Cu surface is reduced.
Nevertheless, more measurements of the plasma treated Cu samples and of the liquid in the discharge chamber have to be done, in order to prove the reproducibility of the Cu nanoparticles. For example pH measurements of the liquid before and after plasma treatment of Cu samples may help to get further information about the reaction chemistry generated by pulsed plasma. Furthermore, Cu samples can be treated with pulsed plasma in aqueous solutions with lower concentration of potassium chloride. This may help to get less nanoparticle clusters and a more cubic nanostructure on the Cu surfaces.

6 Acknowledgement

An dieser Stelle möchte ich mich herzlich bei allen Menschen bedanken, die mich während der Anfertigung meiner Bachelorarbeit unterstützt haben. Ein ganz besonderer Dank geht an

- Prof. Dr. Achim von Keudell, der mir die Möglichkeit gegeben hat, meine Bachelorarbeit an dem Lehrstuhl für Experimentalphysik II zu erstellen.
- Dr. Marc Böke für die hilfreichen Beiträge während der Projektmeetings und für die Bereitstellung zur Zweitkorrektur
- Dr. Ioannis Zegkinoglou, der es mir ermöglicht hat, am Rasterelektronenmikroskop zu arbeiten
- Dr. Marina Prenzel für die stetige Hilfbereitschaft und die vielen Ratschläge
- Katharina Grosse, die mich während der gesamten Zeit sehr gut betreut hat, mir bei Fragen zur Seite stand und sich die Zeit genommen hat, meine Arbeit Korrektur zu lesen
- Sascha Thiemann-Monjé für sein Engagement und das Korrekturlesen meiner Bachelorarbeit
- Philipp Grosse für die Beantwortung aufkommender Fragen, für die Unterstüzung bei der Literaturrecherche und der sehr guten Betreuung in Berlin
- Steffen Schüttler und David Steuer für die angenehme Arbeitsatmosphäre im Büro
- Alle Techniker und Mitarbeiter des Lehrstuhls für Experimetalphysik II als auch des Lehrstuhls für Experimentalphysik IV für die große Hilfsbereitschaft
- Meine Familie und Freunde für die moralische Unterstützung und Motivation während meines Studiums
- Stephan Sehring für die motivierenden Gespräche und das Korrekturlesen meiner Arbeit.

A Additional data

A.1 SEM images of Cu samples

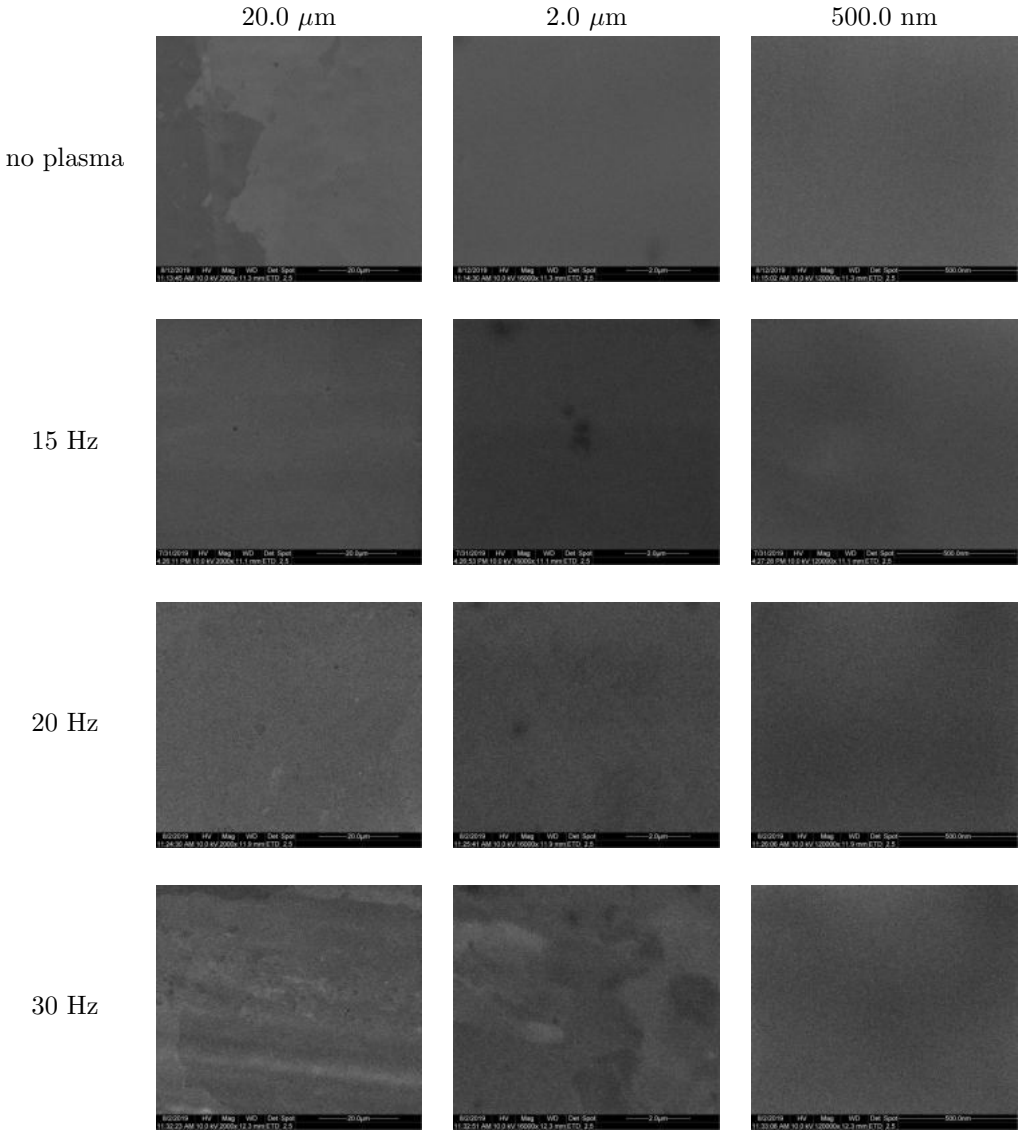

Figure A.1: Frequency variation: Electropolished Cu foils after 20 min of plasma treatment in distilled water are shown. The voltage of the nanosecond pulser is 20 kV and the frequency is given on the left side. The scale bar is on the top. Before plasma treatment water conductivity of 1 μScm^{-1} is measured. Only areas close to the plasma ignition are shown.

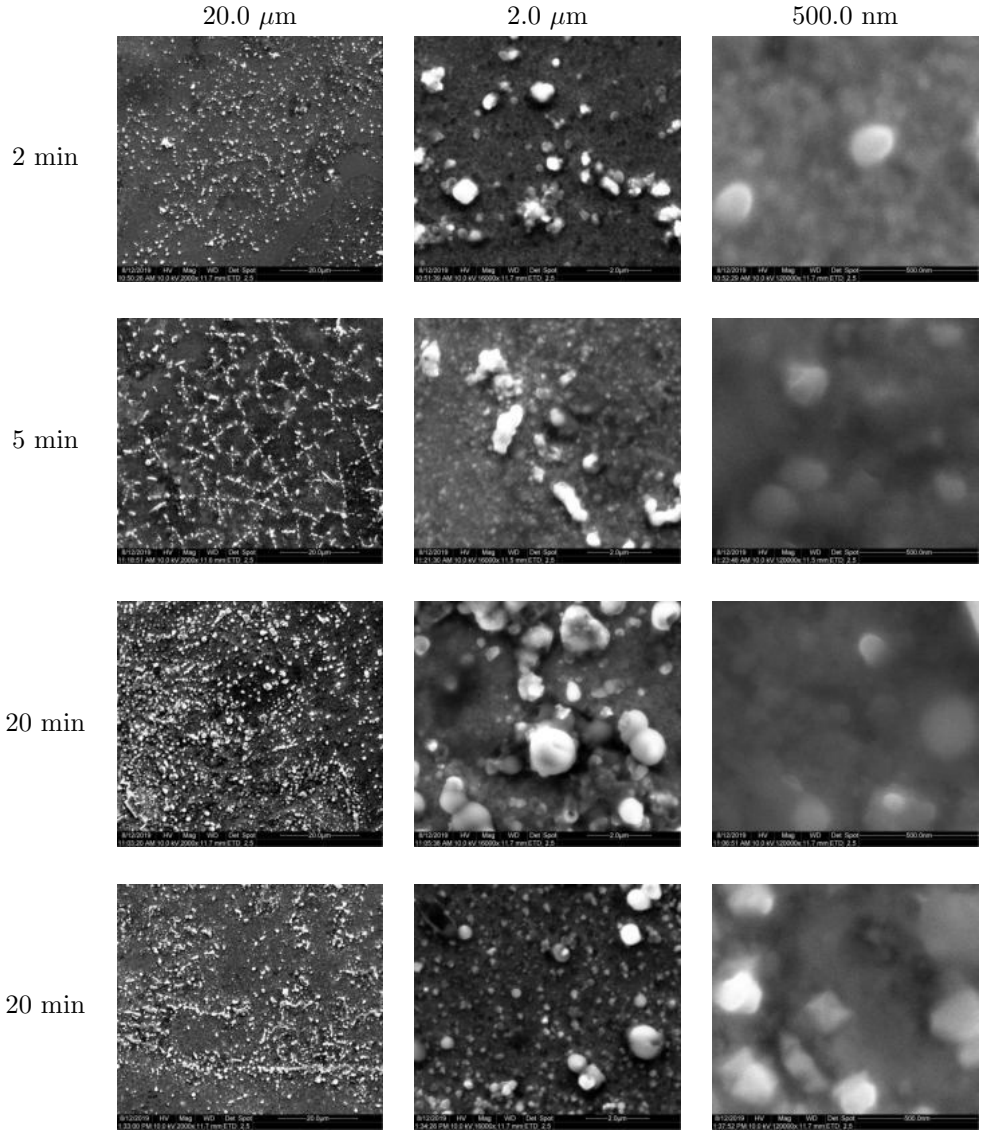

Figure A.2: Time variation: Electropolished Cu foils are treated in 0.0035 M KCl. The treatment time is given on the left side and on the top is the scale bar. The conductivity of the liquid is 568 μScm^{-1} before treatment.

A.2 Experimental setup

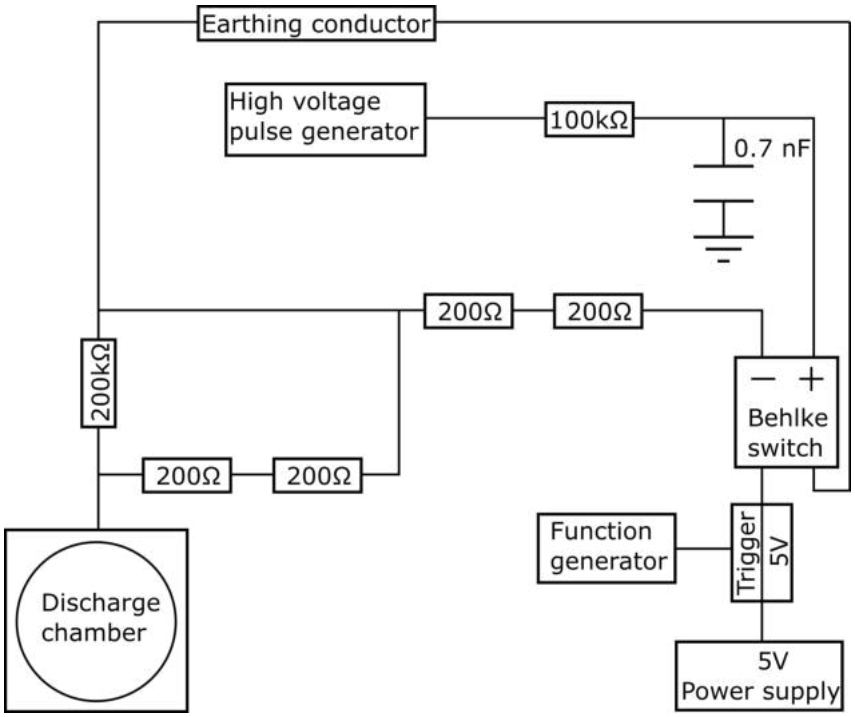

Figure A.3: Experimental setup for the generation of microsecond pulsed plasma in liquid

A.3 Conductivity measurement

U [V]	σ_{H_2O} [μScm^{-1}]		σ_{KCl} [μScm^{-1}]	
	Before	After	Before	After
20	1±1	5±1	568±1	580±1
22	1±1	4±1	568±1	582±1
24	1±1	4±1	568±1	588±1
26	1±1	3±1	568±1	588±1

Table 1: Electrical conductivity of distilled water (σ_{H_2O}) and 0.0035 M KCl (σ_{KCl}) before and after plasma treatment in relation to the applied voltage U at the nanosecond pulse generator which have a frequency of 15 Hz is presented. The distance between both electrodes is (3,7±0,9) mm and the distance between sample and electrode is (3,0±0,7) mm for the measurements of distilled water. The distance between both electrodes is (5,0±0,4) mm and the distance between sample and electrode is (2,5±0,1) mm for the measurements of 0.0035 M KCl.

f [Hz]	σ_{H_2O} [μScm^{-1}]		σ_{KCl} [μScm^{-1}]	
	Before	After	Before	After
15	1±1	8±1	568±1	580±1
20	1±1	9±1	568±1	580±1
30	1±1	7±1	568±1	579±1

Table 2: Electrical conductivity of distilled water (σ_{H_2O}) and 0.0035 M KCl (σ_{KCl}) before and after plasma treatment in relation to the applied frequency f at the nanosecond pulse generator which have a voltage of 20 kV is measured. The distance between both electrodes is (5,0±0,4) mm and the distance between sample and electrode is (2,5±0,1) mm for all measurements.

A.4 Construction of the sample holder

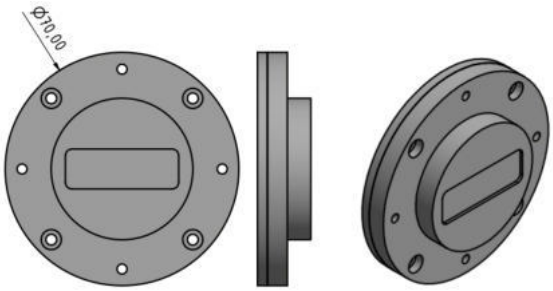

Figure A.4: Construction of the sample holder (private communication with A. von Keudell)

References

[1] M. A. Lieberman and A. J. Lichtenberg, *Principles of Plasma Discharges and Materials Processing*. John Wiley & Sons. Google-Books-ID: m0iOga2XE5wC.

[2] K.-D. Weltmann and T. v. Woedtke, "Plasma medicine—current state of research and medical application," vol. 59, no. 1, p. 014031.

[3] M. Sato, T. Ohgiyama, and J. S. Clements, "Formation of chemical species and their effects on microorganisms using a pulsed high-voltage discharge in water," vol. 32, no. 1, pp. 106–112.

[4] J. Liu, B. He, Q. Chen, H. Liu, J. Li, Q. Xiong, X. Zhang, S. Yang, G. Yue, and Q. H. Liu, "Plasma electrochemical synthesis of cuprous oxide nanoparticles and their visible-light photocatalytic effect," vol. 222, pp. 1677–1681.

[5] R. Akolkar and R. M. Sankaran, "Charge transfer processes at the interface between plasmas and liquids," vol. 31, no. 5, p. 050811.

[6] Q. Chen, J. Li, and Y. Li, "A review of plasma–liquid interactions for nanomaterial synthesis," vol. 48, no. 42, p. 424005.

[7] Q. Chen, J. Li, K. Saito, and H. Shirai, "The characterization of radio-frequency discharge using electrolyte solution as one electrode at atmospheric pressure," vol. 41, no. 17, p. 175212.

[8] S. Horikoshi and N. Serpone, "In-liquid plasma: a novel tool in the fabrication of nanomaterials and in the treatment of wastewaters," vol. 7, no. 75, pp. 47196–47218.

[9] T. A. Kareem and A. A. Kaliani, "Glow discharge plasma electrolysis for nanoparticles synthesis," vol. 18, no. 3, pp. 315–327.

[10] H. Fredriksson, D. Chakarov, and B. Kasemo, "Patterning of highly oriented pyrolytic graphite and glassy carbon surfaces by nanolithography and oxygen plasma etching," vol. 47, no. 5, pp. 1335–1342.

[11] H. Mistry, A. S. Varela, C. S. Bonifacio, I. Zegkinoglou, I. Sinev, Y.-W. Choi, K. Kisslinger, E. A. Stach, J. C. Yang, P. Strasser, and B. R. Cuenya, "Highly selective plasma-activated copper catalysts for carbon dioxide reduction to ethylene," vol. 7, no. 1, pp. 1–9.

[12] E. B. Nursanto, H. S. Jeon, C. Kim, M. S. Jee, J. H. Koh, Y. J. Hwang, and B. K. Min, "Gold catalyst reactivity for CO2 electro-reduction: From nano particle to layer," vol. 260, pp. 107–111.

[13] B. Roldan Cuenya, "Metal nanoparticle catalysts beginning to shape-up," vol. 46, no. 8, pp. 1682–1691.

[14] D. Gao, I. Zegkinoglou, N. J. Divins, F. Scholten, I. Sinev, P. Grosse, and B. Roldan Cuenya, "Plasma-activated copper nanocube catalysts for efficient carbon dioxide electroreduction to hydrocarbons and alcohols," vol. 11, no. 5, pp. 4825–4831.

[15] R. Reske, H. Mistry, F. Behafarid, B. Roldan Cuenya, and P. Strasser, "Particle size effects in the catalytic electroreduction of CO2 on cu nanoparticles," vol. 136, no. 19, pp. 6978–6986.

[16] H. Mistry, R. Reske, Z. Zeng, Z.-J. Zhao, J. Greeley, P. Strasser, and B. R. Cuenya, "Exceptional size-dependent activity enhancement in the electroreduction of CO2 over au nanoparticles," vol. 136, no. 47, pp. 16473–16476.

[17] H. Mistry, F. Behafarid, R. Reske, A. S. Varela, P. Strasser, and B. Roldan Cuenya, "Tuning catalytic selectivity at the mesoscale via interparticle interactions," vol. 6, no. 2, pp. 1075–1080.

[18] W. Tang, A. A. Peterson, A. Sofia Varela, Z. P. Jovanov, L. Bech, W. J. Durand, S. Dahl, J. K. Nørskov, and I. Chorkendorff, "The importance of surface morphology in controlling the selectivity of polycrystalline copper for CO2 electroreduction," vol. 14, no. 1, pp. 76–81.

[19] O. A. Baturina, Q. Lu, M. A. Padilla, L. Xin, W. Li, A. Serov, K. Artyushkova, P. Atanassov, F. Xu, A. Epshteyn, T. Brintlinger, M. Schuette, and G. E. Collins, "CO2 electroreduction to hydrocarbons on carbon-supported cu nanoparticles," vol. 4, no. 10, pp. 3682–3695.

[20] K. Manthiram, B. J. Beberwyck, and A. P. Alivisatos, "Enhanced electrochemical methanation of carbon dioxide with a dispersible nanoscale copper catalyst," vol. 136, no. 38, pp. 13319–13325.

[21] C. Shou Chen, A. D. Handoko, J. Hui Wan, L. Ma, D. Ren, and B. Siang Yeo, "Stable and selective electrochemical reduction of carbon dioxide to ethylene on copper mesocrystals," vol. 5, no. 1, pp. 161–168.

[22] F. S. Roberts, K. P. Kuhl, and A. Nilsson, "High selectivity for ethylene from carbon dioxide reduction over copper nanocube electrocatalysts," vol. 54, no. 17, pp. 5179–5182.

[23] S. Sen, D. Liu, and G. T. R. Palmore, "Electrochemical reduction of CO2 at copper nanofoams," vol. 4, no. 9, pp. 3091–3095.

[24] W. Zhu, Y.-J. Zhang, H. Zhang, H. Lv, Q. Li, R. Michalsky, A. A. Peterson, and S. Sun, "Active and selective conversion of CO2 to CO on ultrathin au nanowires," vol. 136, no. 46, pp. 16132–16135.

[25] Q. Lu, J. Rosen, and F. Jiao, "Nanostructured metallic electrocatalysts for carbon dioxide reduction," vol. 7, no. 1, pp. 38–47.

[26] B. Khezri, A. C. Fisher, and M. Pumera, "CO 2 reduction: the quest for electrocatalytic materials," vol. 5, no. 18, pp. 8230–8246.

[27] S. K. S. Gupta, "Contact glow discharge electrolysis: its origin, plasma diagnostics and non-faradaic chemical effects," vol. 24, no. 6, p. 063001.

[28] I. Langmuir, "Oscillations in ionized gases," vol. 14, no. 8, pp. 627–637.

[29] F. F. Chen, *Introduction to plasma physics and controlled fusion*, vol. 1. Springer.

[30] P. Bruggeman and C. Leys, "Non-thermal plasmas in and in contact with liquids," vol. 42, no. 5, p. 053001.

[31] G. Saito and T. Akiyama, "Nanomaterial synthesis using plasma generation in liquid."

[32] P. Šunka, "Pulse electrical discharges in water and their applications," vol. 8, no. 5, pp. 2587–2594.

[33] H. Akiyama, "Streamer discharges in liquids and their applications," vol. 7, no. 5, pp. 646–653.

[34] W. An, K. Baumung, and H. Bluhm, "Underwater streamer propagation analyzed from detailed measurements of pressure release," vol. 101, no. 5, p. 053302.

[35] K. Schoenbach, J. Kolb, S. Xiao, S. Katsuki, Y. Minamitani, and R. Joshi, "Electrical breakdown of water in microgaps," vol. 17, no. 2, p. 024010.

[36] J. C. Devins, S. J. Rzad, and R. J. Schwabe, "Breakdown and prebreakdown phenomena in liquids," vol. 52, no. 7, pp. 4531–4545.

[37] K. Grosse, J. Held, M. Kai, and A. v. Keudell, "Nanosecond plasmas in water: ignition, cavitation and plasma parameters," vol. 28, no. 8, p. 085003.

[38] A. R. Denaro and A. Hickling, "Glow-discharge electrolysis in aqueous solutions," vol. 105, no. 5, pp. 265–270.

[39] S. K. Sengupta, R. Singh, and A. K. Srivastava, "A study on the origin of nonfaradaic behavior of anodic contact glow discharge electrolysis the relationship between power dissipated in glow discharges and nonfaradaic yields," vol. 145, no. 7, pp. 2209–2213.

[40] P. Bruggeman, F. Iza, D. Lauwers, and Y. A. Gonzalvo, "Mass spectrometry study of positive and negative ions in a capacitively coupled atmospheric pressure RF excited glow discharge in he–water mixtures," vol. 43, no. 1, p. 012003.

[41] P. Pootawang, N. Saito, and S. Y. Lee, "Discharge time dependence of a solution plasma process for colloidal copper nanoparticle synthesis and particle characteristics," vol. 24, no. 5, p. 055604.

[42] L. D. Menard, F. Xu, R. G. Nuzzo, and J. C. Yang, "Preparation of TiO2-supported au nanoparticle catalysts from a au13 cluster precursor: Ligand removal using ozone exposure versus a rapid thermal treatment," vol. 243, no. 1, pp. 64–73.

[43] J.-J. Zou, C.-J. Liu, and Y.-P. Zhang, "Control of the metal-support interface of NiO-loaded photocatalysts via cold plasma treatment," vol. 22, no. 5, pp. 2334–2339.

[44] L. K. Ono and B. Roldan Cuenya, "Formation and thermal stability of au2o3 on gold nanoparticles: Size and support effects," vol. 112, no. 12, pp. 4676–4686.

[45] Y. Zhou, T. Holme, J. Berry, T. R. Ohno, D. Ginley, and R. O'Hayre, "Dopant-induced electronic structure modification of HOPG surfaces: Implications for high activity fuel cell catalysts," vol. 114, no. 1, pp. 506–515.

[46] *Technician's PHI5000 System Hardware Manual*.

[47] J. F. Moulder, W. F. Stickle, and P. E. Sobol, *Handbook of X-ray photoelectron spectroscopy: a reference book of standard spectra for identification and interpretation of XPS data*. Physical Electronics, Inc. OCLC: 925632097.

[48] J. I. Goldstein, D. E. Newbury, J. R. Michael, N. W. M. Ritchie, J. H. J. Scott, and D. C. Joy, *Scanning Electron Microscopy and X-Ray Microanalysis*. Springer-Verlag, 4 ed.

[49] C. Nenbangkaeo, "Analysis of hydrogen peroxide production in nanosecond pulsed discharges in water," 2019.

[50] N. T. K. Thanh, N. Maclean, and S. Mahiddine, "Mechanisms of nucleation and growth of nanoparticles in solution," vol. 114, no. 15, pp. 7610–7630.

[51] M. C. Biesinger, "Advanced analysis of copper x-ray photoelectron spectra," vol. 49, no. 13, pp. 1325–1334.

[52] I. Moussallem, J. Jörissen, U. Kunz, S. Pinnow, and T. Turek, "Chlor-alkali electrolysis with oxygen depolarized cathodes: history, present status and future prospects," vol. 38, no. 9, pp. 1177–1194.

[53] G. Saito, S. Hosokai, M. Tsubota, and T. Akiyama, "Synthesis of copper/copper oxide nanoparticles by solution plasma," vol. 110, no. 2, p. 023302.

[54] "Kupferoxide - RÖMPP, thieme."

[55] I. L. Soroka, A. Shchukarev, M. Jonsson, N. V. Tarakina, and P. A. Korzhavyi, "Cuprous hydroxide in a solid form: does it exist?," vol. 42, no. 26, pp. 9585–9594.